2m'4

EARTH'S GRAVITY FIELD TO THE EIGHTEENTH DEGREE AND
GEOCENTRIC COORDINATES FOR 104 STATIONS FROM SATELLITE
AND TERRESTRIAL DATA[*]

E. M. Gaposchkin

Center for Astrophysics

Harvard College Observatory and Smithsonian Astrophysical Observatory

and

Center for Earth and Planetary Physics

Harvard University

Cambridge, Massachusetts 02138

Short title: Earth's Gravity Field

404-065

ABSTRACT

Geodetic parameters describing the earth's gravity field and the positions of satellite-tracking stations in a geocentric reference frame have been computed. These parameters were estimated by means of a combination of five different types of data: routine and simultaneous satellite observations, observations of deep-space probes, measurements of terrestrial gravity, and surface-triangulation data. The combination gives better parameters than does any subset of data types. The dynamic solution used precision-reduced Baker-Nunn observations and laser range data of 25 satellites. Data from the 49-station National Oceanic and Atmospheric Administration BC-4 network, the 19-station Smithsonian Astrophysical Observatory Baker-Nunn network, and independent camera stations were employed in the geometrical solution. Data from the tracking of deep-space probes were converted to relative longitudes and distances to the earth's axis of rotation of the tracking stations. Surface-gravity data in the form of 550-km squares were derived from 19,328 $1° \times 1°$ mean gravity anomalies. The surface-triangulation data consisted of the datum coordinates of each tracking station. Coordinates and potential coefficients were derived separately for each iteration. The adopted solution in each iteration was a combination solution chosen to improve the residuals of all data types. In addition to these five data sets, an independent test of the solution utilized sea-level heights plus satellite-tracking and surface-gravity data not used in the combination. The total gravity field is represented by spherical-harmonic coefficients complete to degree and order 18 and a number of higher degree terms. The half-wavelength resolution of this global solution subtends about 10° at the earth's center. The accuracy of the global gravity field has been estimated as ± 2.5 m in geoid height, or 64 mgal^2. Coordinates of the fundamental laser stations are determined with an accuracy of 2 to 4 m, and those of the fundamental optical network, of 5 to 10 m. The best-fitting ellipsoid has a flattening f of $1/f = 298.256 \pm 0.001$ and a semimajor axis $a_e = 6378140.4 \pm 1.2$ m.

1. INTRODUCTION

The Smithsonian Astrophysical Observatory (SAO) has published a series of
Standard Earth (SE) models based on satellite-tracking and other data (Kozai, 1964,
1969; Gaposchkin, 1967, 1970; Köhnlein, 1967; Veis, 1967a, b; Whipple, 1967;
Lundquist and Veis, 1966 (hereafter referred to as SE I); Lambeck, 1969, 1970;
Gaposchkin and Lambeck, 1970 (referred to as SE II). There has been a steady
advance in the accuracy of the analytical treatment, the accuracy and completeness
of the data, and the significance of the results. The results summarized here are a
continuation of Gaposchkin and Lambeck (1970); they were reported at the American
Geophysical Union Meeting in April 1973 and at the First International Symposium
for the Use of Artificial Satellites for Geodesy and Geodynamics in May 1973 and
have been published in Gaposchkin (1973; referred to as SE III).

Each Standard Earth model consists of 1) a set of geocentric coordinates for
stations observing satellites and 2) a set of spherical harmonics representing the
geopotential. These two sets of unknowns can be correlated in the least-squares
adjustment, and both sets of parameters have been determined in the same computa-
tion. This led, for example in Gaposchkin and Lambeck (1970), to solving a system
with 428 unknowns -- i.e., for 39 stations and gravity-field coefficients complete
through degree and order 16. Evaluation of the Gaposchkin and Lambeck (1970) results
indicated that the remaining errors in these parameters were small; that is, the
corrections to the parameters would be small. Therefore, the effect of errors in
the adopted station coordinates on the determination of the gravity field, and vice
versa, would be small, and the two sets of parameters could be computed separately.

A general revision of the parameters for SE III was undertaken because of
new and improved data for almost all types of observations. Optical satellite
observations have been augmented by a large body of laser data with global coverage
from the International Satellite Geodesy Experiment (ISAGEX). Two satellites with
inclinations significantly lower (5° and 15°) than previously available have been launched

since 1970. Available surface-gravity data have been significantly improved by the distribution of a compilation of gravity anomalies by the Aeronautical Chart and Information Center (ACIC). Determinations of station coordinates have been improved by data from the worldwide BC-4 geometrical network. Finally, information on site locations from the Deep Space Net (DSN) of the Jet Propulsion Laboratory (JPL) has been revised with the addition of new data and improved processing techniques.

The analysis was divided into two parts because of the initial high accuracy of the geodetic parameters, the good coverage of all types of observational material, and the result from Gaposchkin and Lambeck (1970) indicating that the interaction between the gravity field and the station coordinates is relatively small. The determinations of the gravity field and of station coordinates were carried out in parallel, described in Gaposchkin, Williamson, Kozai, and Mendes (1973) and in Gaposchkin, Latimer, and Veis (1973), respectively. In an iterative process, the improved coordinates were used in the next iteration for the gravity field, and then the improved gravity field was used in the subsequent iteration for the station coordinates. This process, known as the block Gauss-Seidel iteration, will rigorously converge.

Gaposchkin (1970) has shown that, except for isolated harmonics, the gravity field beyond 18th or 20th degree has a negligible effect on a satellite. The only exceptions are some zonal harmonics that give rise to secular and long-period effects, and the resonant harmonics. Therefore, one cannot hope to obtain from analysis of satellite perturbations much more detail beyond 16th degree and order than is already available. Greater detail will have to come from other methods, such as terrestrial gravimetry. The purpose here is to improve those harmonics to which satellite orbits are sensitive. Many of the harmonics between 10th and 18th degree are not very well determined from satellite-perturbation analysis, but terrestrial gravimetry, when combined with satellite data, provides a good determination of these coefficients.

Since the gravity field beyond 18th degree does not give rise to an observable change in satellite position, the satellite observations could be modeled with the use of a gravity field complete through degree and order 18, including, of course, some additional resonant and zonal harmonics. Therefore, there is no model error due to neglected higher harmonics. However, the surface-gravity data are given in area means of 550 km $\times$ 550 km squares. This surface distribution of gravity would require a spherical-harmonic development to $\ell = m = 36$. Therefore, using a gravity field

through degree and order 18 will have a significant model error that must be taken into account in establishing weights and making comparisons with surface-gravity data.

A number of approaches can be used to determine the position of points on the earth's surface. Of these, we have chosen tracking of close-earth satellites, deep-space probes, and surface-triangulation measurements for this analysis. The data and the method of analysis have been selected to optimize the results for a global network of reference points.

The satellite methods separate nicely into two distinct types of analysis: geometrical and dynamical. The former hinges on making simultaneous observations of a satellite from two or more points on the earth's surface. When these are camera observations, the vector connecting the two stations must lie in the plane defined by the two observed directions. A number of independent simultaneous observations will define the direction between the two stations. SAO has obtained a sufficient number of simultaneous observations to determine a network for its stations. The National Ocean Survey (NOS) of the National Oceanic and Atmospheric Administration (NOAA) has carried out a program of observations with the BC-4 camera to establish a global geometrical network. Figure 1 shows the distribution of observing stations included in SE III.

The dynamical analysis assumes the satellite's orbit is known and computes the location of the observing station from individual observations. In practice, the orbit is determined from the same observations. The orbital mode has been used by SAO to analyze tracking data on close-earth satellites and by JPL to analyze tracking data on deep-space probes.

Surface-triangulation measurements are reduced by organizations such as NOS and the Defense Mapping Agency, who publish coordinates of given points referred to a datum that, in general, has an arbitrary origin, orientation, and scale. The relative positions of stations are determined from these data.

The main objectives of this analysis are the following:

A. To improve the low-degree and low-order harmonics from satellite data and the higher degree and order harmonics from terrestrial data.

B. To improve the accuracy of the fundamental stations. Heretofore (SE II), the accuracy was estimated as 5 to 10 m.

C. To improve the distribution of reference points or tracking sites. In SE II, coordinates were obtained for 39 independent sites.

D. To use the latest available data. New data include the complete BC-4 network and all the laser tracking data taken during the ISAGEX program. Surface-triangulation data were used as observations rather than as constraints.

2. DATA AVAILABLE

2.1 Satellite Data Collection, Reduction, and Reference System

In addition to data from the Baker-Nunn and laser networks, we also used the following data collected by other agencies (see Figure 1):

A. Laser data from stations 7804, 7809, 7815, 7816, and 7818 were made available by the Centre National d'Etudes Spatiales (CNES) in France.

B. Goddard Space Flight Center (GSFC) provided laser data from stations 7050 and 7060.

C. Simultaneous observations of the Pageos satellite taken by the BC-4 camera network were made available by the NOS of NOAA.

D. Optical data were obtained from the following European stations: 8015 and 8019 (Observatoire de Paris), 9066 (Astronomical Institute, Bern), 9074 and 9077 (USSR Astronomical Council), and 9080 (Royal Radar Establishment, Malvern).

E. Reduced deep-space-probe data from DSN stations 4711, 4712, 4714, 4741, 4742, 4751, 4761, and 4762 were provided by JPL of the California Institute of Technology.

All the satellites used in the orbit computation are listed in Table 1, and Figure 2 shows their distribution in inclination and height. In the determination of station coordinates, high satellites less affected by the anomalous gravity field were emphasized. Specifically, we eliminated satellites with drag model errors (large area-to-mass ratio and low perigee height), particular sensitivity to gravity-field model errors (resonances), or poor orbital distribution (less than six stations observing the satellite). Certain satellites with unmanageable long-period resonances (e.g., 5900701) were used only for the determination of station coordinates; they have such a rich body of data that relatively short-arc orbits (4 days) could be derived for this purpose. For the determination of the gravity field, lower satellites with a more uniform distribution in inclination were stressed.

The optical data that were reduced included all terms in precession and nutation necessary to ensure that the maximum neglected effect was less than 0.5 m. We applied annual aberration to all observations and diurnal aberration to the simultaneous observations. Parallactic refraction was applied by use of mean nighttime temperature and pressure taken at each station to calculate the refraction coefficient (Gaposchkin, 1972). Systematic corrections to star-catalog positions were applied where appropriate. All optical data received from other agencies were corrected in the same way. The accuracy of the optical data ranges from 1 to 4".

The laser range data are considered to be accurate to about 2 m and are reduced by use of the corrections described in Lehr (1969). The influence of timing errors at the stations also has to be considered. For passes with more than 30 observed points, we selected 30 points equally spaced in the pass. To account for redundancy and systematic errors of the laser data, the assumed accuracy of each laser point was modified as indicated in Table 9 (see Section 3.2) for the determination of coordinates and in Table 21 (see Section 4.3) for the determination of the geopotential.

SAO has its own master clock and, through VLF transmission, maintains its own coordinated time system, called A.S. The principal time reductions were to convert the GSFC data from UTC to A.S and the CNES data from A3 to A.S. It is assumed that atomic time is a satisfactory system for ephemeris calculation and that the error in observing time is random.

The analysis assumes that the stations for a fixed system (i.e., there is no relative motion due, for example, to tides or crustal movements) and the pole position and instantaneous position of the earth are known without error from numerical values published by the International Polar Motion Service (IPMS) and the Bureau International de l'Heure (BIH). It appears that these data may be a limiting factor for the ultimately attainable accuracy of station positions. Polar-motion data from IPMS differ from those published by the BIH by as much as 1.5 m for the period since the two systems have been referred to the same origin. The IPMS data used here were all referred to the mean pole of 1900-1905, and the coordinate system is the equator of date and the equinox of 1950.0. We have assumed that the BC-4 camera data are referred to the terrestrial system through the same values of pole position and UT1.

2.2 Information from Deep-Space Probes

Data from DSN's eight-station network for tracking deep-space probes have been used to obtain, among other parameters, the longitudes (relative and absolute) of each station and the distance of its antenna to the earth's instantaneous axis of rotation (Vegos and Trask, 1967; Trask and Vegos, 1968). The DSN data are particularly interesting because 1) they constitute a unique, complementary, and independent determination of geocentric locations, and 2) they provide a very strong determination of scale.

Comparisons of the JPL and SAO results have been made by Veis (1966) and Vegos and Trask (1967) from data from the Ranger missions and from SE I (Lundquist and Veis, 1966). More refined JPL solutions were combined with satellite-tracking data in the determination of SE II. The combination was made with Location Set (LS) 25, as determined by Mottinger (1969), by using data from the Mariner 4 and 5 missions. Continued refinement of the DSN data has provided LS 37, which is used in the present analysis (Mottinger, 1973).

Each DSN site is located near other stations whose coordinates were determined in the analysis presented here. Surface-triangulation data, in the form of geodetic coordinates, can be used to relate the DSN coordinates to the SAO coordinates.

The ephemeris r of a deep-space probe is assumed known. For a distant spacecraft, the observed range rate $\dot{\rho}$ can be expressed approximately as

$$\dot{\rho} = \dot{r} + \omega r_s \cos \delta \sin (\alpha_s - \alpha_0) \quad ,$$

where ω is the earth's rotation rate, r_s is the spin-axis distance of the observer, δ and α_0 are the declination and right ascension of the spacecraft, and α_s is the right ascension of the observer. Each station observes a diurnal variation in $\dot{\rho}$, the amplitude and phase depending on r_s and α_s, respectively.

Generally, any data can be analyzed. However, cruise data seem less reliable than close-encounter data for determining α_s (Mottinger, 1973), and they are used only for the determination of r_s. In any case, refraction (tropospheric and ionospheric) and orbit computation must be done with great care, and recent improvements come from refinements in the treatment of refraction. The ephemeris r (δ, α_0) will be determined in the system of the JPL planetary ephemeris. We can expect to find a systematic difference in the definition of longitude between the planetary ephemeris and the astronomical reference system (FK4) used for analysis of close-earth satellites. The DSN data reduction used numerical values for pole position and UT1 from BIH, as was done for the close-earth-satellite analyses.

The data for LS 37 are summarized in Table 2. The main improvements over LS 25 are as follows:

A. Better treatment of refraction, particularly ionospheric.

B. Inclusion of more data because of A.

C. Inclusion of Mariner 6 encounter data.

D. Revision of the planetary ephemeris.

E. Use of BIH polar motion and UT1.

Realistic estimates of accuracy are 2 m for r_s, 4 m for absolute longitude, and 2 m for relative longitude (Mottinger, 1972).

Mottinger (1972) provided a solution and covariance matrix for r_s, λ, in addition to the masses of Venus, Mars, and the moon and the oblateness of Mars. This system was transformed by SAO for corrections in coordinates X, Y of the station. These converted equations were then added to the larger system of normal equations, which included the other stations sought.

The LS 37 coordinates for the DSN stations are given in Table 3. In LS 37, the relative coordinates of 4711, 4712, and 4714 and of 4761 and 4762 were constrained to agree with the survey data.

2.3 Information from Surface Triangulation

Extensive surface-triangulation data exist that relate station positions. These data are generally given in terms of datum coordinates and occasionally in terms of interstation vectors for collocated stations. We have used this information in four ways:

A. For stations in the same datum, the geodetic coordinates are used as observations relating the positions of the stations in the general combination adjustment.

B. For collocated instruments, these datum coordinates are used as a constraint relating the two sites. These cases could be treated as in A above.

C. The geodetic coordinates are utilized as a check on the accuracy of the final coordinates.

D. The geodetic coordinates are employed to determine the relation of each datum to a geocentric reference system.

Evaluating geodetic coordinates is the most difficult aspect of this analysis. When reliable, they are very accurate; but problems often exist in relating the local survey at the station to the datum.

In A, B, and C above, care must be taken to ensure that datum tilts, distortions, and scale differences do not corrupt the results. For most uses, limiting the application of geodetic coordinates to lengths of 100 km or less is satisfactory. Otherwise, the datum orientation must be determined and applied before the geodetic coordinates can be used with geocentric satellite-based coordinates.

The use of datum coordinates as observations of relative station positions assumes no correlation between X, Y, and Z. If we have datum coordinates for station i, X_i^d, Y_i^d, Z_i^d, and initial values for the geocentric coordinates that are to be corrected, X_i^g, Y_i^g, Z_i^g, we can write observation equations for each component of the vector between two stations:

$$X_i^d - X_j^d = X_i^g - X_j^g + \Delta X_i - \Delta X_j \quad ,$$

with similar expressions for Y and Z. If these are given weights W_{ij}, we can immediately write the normal system as

$$
\begin{bmatrix}
\sum\limits_{i} \sigma_{ij} & \cdots & -\sigma_{ij} \\
\vdots & \vdots & \vdots \\
-\sigma_{ij} & \cdots & \sum\limits_{j} \sigma_{ij}
\end{bmatrix}
\begin{bmatrix}
\Delta X_i \\
\vdots \\
\Delta X_j
\end{bmatrix}
=
\begin{matrix}
\sum\limits_{i} \sigma_{ij} \left[\left(X_i^d - X_j^d \right) - \left(X_i^g - X_j^g \right) \right] \\
\\
\sum\limits_{j} \sigma_{ij} \left[\left(X_j^d - X_i^d \right) - \left(X_j^g - X_i^g \right) \right]
\end{matrix},
$$

where $\sigma_{ij} = (1/W_{ij})^2$. This system can augment a normal system for determining ΔX, ΔY, ΔZ.

The accuracy W_{ij} of the geodetic ties chosen is given in Table 4 (see Gaposchkin, 1973, for the geodetic coordinates of all the stations used in SE III).

2.4 Terrestrial Gravity Data

The primary objective of the analysis of terrestrial gravity data is to obtain mean anomalies for regions 550 km × 550 km. When these data are combined with the satellite-perturbation analysis, the spherical harmonics representing the geopotential can be determined. A set of gravity data with known (and preferably simple) statistical properties is needed. Our approach is based on covariance analysis, following the ideas of Wiener (1966) and Kolmogoroff. When this technique is used in communications engineering, it is sometimes known as filtering theory. The ideas here are an extension of a one-dimensional time series to the two-dimensional surface of a sphere (Kaula, 1967).

Estimation of gravity by covariance methods hinges on the stationarity of gravity data; that is, the statistical properties of the data are the same no matter where the data are taken. There is some evidence that gravity data are not stationary; however, if some subsets of the total gravity population are stationary, then gravity covariance functions between sets and within each set can be defined (see Gaposchkin, 1973, for details).

A set of $1° \times 1°$ mean free-air anomalies, containing 19,115 measured means, was obtained from ACIC (1971), and another set, of 1454 $1° \times 1°$ means for Australia, from Mather (1970). The two sets were combined, with the Mather data being used for all areas they covered. Figure 3 shows the geographical coverage of all the data. The combined data set contained 19,328 means. A complete set of $1° \times 1°$ mean topographic heights, used to define oceanic and continental areas, was obtained from Kaula (Kaula and Lee, 1967). The distribution of $1° \times 1°$ mean gravity data is summarized in Table 5.

The estimated uncertainty given with each gravity anomaly for 99.9% of the data is less than 25 mgal. Comparing the Mather data with the ACIC data at the 1241 common points, we find that the average difference is 1.7 mgal and the root-mean-square (rms) difference is 20 mgal. At a number of points, the discrepancy between the two sets exceeds 100 mgal.

Kaula (1967) has developed a procedure that greatly simplies the calculation of the covariance function, which is called the block covariance function, and the gravity estimates. This method has both advantages and disadvantages. The disadvantages follow:

A. The estimate of gravity does not make use of all the gravity information; i.e., the estimates are not so good as possible.

B. The covariance function must be determined by using only the combinations of anomalies within blocks and therefore does not employ all possible combinations of the data.

The advantages of Kaula's method are as follows:

A. It greatly simplifies calculation of the covariance function and the gravity estimates.

B. It produces mean anomalies $550 \text{ km} \times 550 \text{ km}$ with uncorrelated errors.

C. The statistical properties of data within a block may be closer to stationarity since the method involves primarily the short-distance covariance.

If the gravity signal were a stationary process, then it would have the same statistical properties everywhere. Possible nonstationarity has been investigated.

The main result is that by using the block covariance estimator of Kaula, a statistically independent set of 550 km × 550 km averages is obtained with no loss of accuracy. Block covariance provides the optimum set of gravity anomalies when used in combination with satellite observations. Table 6 and Figure 4 present the global covariance function for the 1° × 1° mean gravity anomalies. In Table 7 and Figure 5, we give the block covariance function, and in Table 8, the covariance function of the derived 550 km × 550 km anomalies. The reader is referred to Gaposchkin (1973) for a list of the derived anomalies used in combination with satellite data for the determination of the geopotential.

The gravity anomalies are given with respect to the international gravity formula (Heiskanen and Moritz, 1967, p. 79) and must be corrected to refer to the best-fitting ellipsoid defined by J_2 and the adopted values of a_e, GM, and ω_e. We must also include the Potsdam correction of -14 mgal. Using the following initial values:

$$J_2 = 1082.637 \quad ,$$

$$a_e = 6.378140 \times 10^8 \text{ cm} \quad ,$$

$$GM = 3.986013 \times 10^{20} \text{ cm}^3 \text{ sec}^{-2} \quad ,$$

and

$$\omega_e = 7.292115085 \times 10^{-5} \text{ sec}^{-1} \quad ,$$

we have

$$1/f = 298.256 \quad ,$$

and the correction

$$\delta g_{SAO} - \delta g_{int} = 1.3 - 13.8 \sin^2 \phi \text{ mgal} \quad .$$

3. DETERMINATION OF STATION COORDINATES

3.1 Geometrical Solution

In deriving a geometrical solution, the objective was to produce a system of normal equations for use in combination with other data. The data consisted of direction observations only, and there is no scale information in the geometric net. Nor is there any information to locate the origin of a geometrical network. Hence, any purely geometrical solution with these data would require an arbitrary scale and origin. The combination of normal systems avoids this problem, as other data sets contain scale and origin information. The result of an unscaled, purely geometrical solution is a set of interstation directions, independent of the arbitrary scale and origin introduced.

The geometrical solution included two networks: 27 stations of the SAO network, including the U. S. Air Force Baker-Nunn cameras and several European stations; and 48 stations of the NOS BC-4 network. Of the SAO group, 21 stations were also included in the dynamical solution. The SAO data block consisted of 5200 pairs of synthetic simultaneous observations, or about 50,000 individual direction observations processed at SAO. The satellites observed were 6102801 (Midas 4), 6303004, 6508901 (Geos 1), 6605601 (Pageos), 6800201 (Geos 2), and 6305501. The BC-4 data consisted of 2157 pairs of simultaneous events of Pageos. Each event generally consisted of seven directions and a covariance matrix from each of two stations. When more than two stations observed the satellite simultaneously, we treated each station pair separately.

The computation was divided into two stages. First, all data between pairs of stations were used to determine, by least squares, the interstation direction and its covariance matrix for each pair. The mathematical model for determining this direction uses the condition that the interstation direction (u_3) and the two directions from the stations to the satellite (u_1, u_2) must be coplanar:

$$\hat{u}_1 \cdot \hat{u}_2 \times \hat{u}_3 = 0 \quad . \tag{1}$$

A system of first-order Taylor expansion approximations to equation (1) is solved by least squares to determine u_3 and its 2×2 covariance matrix. In order for truly simultaneous points (u_1, u_2) to be obtained, synthetic observations were computed by interpolation from a series of observations overlapping in time from two stations (Aardoom, Girnius, and Veis, 1966). The synthetic observations (u_1, u_2) are weighted according to the quadratic fit of the individual observations used to determine the synthetic ones. The weight is modified according to SE II (p. 8) to account for the possibility of systematic errors, principally in station timing. Separate synthetic observations are considered to be uncorrelated. For BC-4 data, the NOS has derived seven simultaneous observations from each photographic plate (event) with the associated 14×14 covariance matrix for each set of directions. These are the data provided and used to determine u_3. For the SAO block, 68 directions were determined, and for the BC-4 group, 152.

The second stage consisted of a network adjustment for each data block. The mathematical model for stage two is that of variation of coordinates:

$$\vec{u}_1 - \vec{u}_2 - \vec{u}_3 = 0 \quad ,$$

where $\vec{u}_1$ is the vector from station 1 to the satellite, $\vec{u}_2$ is that from station 2 to the satellite, and $\vec{u}_3$ is the interstation vector. Satellite positions are eliminated, and we obtain a solution for station coordinates, thus deriving adjusted interstation directions. This is equivalent to adjusting the directions directly by using the coplanarity condition for each triangle formed by observed directions between three stations. The advantage of this normal system is that it refers to coordinates, not directions, and can be readily combined with other normal systems for station coordinates. These directions are given in Gaposchkin (1973).

We have available for comparison the interstation directions and their accuracy estimates σ_1^2 resulting from simultaneous-observation data and also the new directions and accuracy estimates σ_2^2 resulting from the network adjustment. Gaposchkin (1973) gives accuracy estimates for interstation vectors.

We expect that, on the average, for the interstation direction adjustment δ,

$$\delta^2 \leq (\sigma_1^2 + \sigma_2^2)/2 .$$

To satisfy this condition, we must multiply the variance estimates by a factor

$$k^2 = \frac{\delta^2}{(\sigma_1^2 + \sigma_2^2)/2}$$

The average value for k^2 is 2.65, and the accuracy estimates for the geometrical solution are scaled by this number. A similar analysis of the BC-4 network gives an average value for k^2 of 2.60.

3.2 Dynamical Solution

An observation $\mathcal{O}$ of direction (right ascension and declination) or range can be related to the satellite position $\bar{r}(t)$ and to the station position $\bar{X}$ by

$$\mathcal{O} = [A] [\bar{r}(t) - R(\theta, x, y) \bar{X}] \tag{2}$$

In general, A is an easily computed transformation matrix. Further, the orbit $\bar{r}(t)$ depends on the orbital elements, the gravity field, the atmospheric density, solar and lunar gravitational attraction, and radiation pressure. Finally, equation (2) depends on UT1 – i.e., the sidereal angle θ – and on the pole position x and y. None of these quantities is known without error and each, in itself, provides a number of difficult problems. For a certain class of satellites, the earth's gravity field presents the major source of error but is improved as part of the analysis described here.

Two types of data have been used in the dynamical solution. Observations of direction are made by photographing the satellite against a star background. The star positions then define the direction from the observing station to the satellite in the coordinates of right ascension and declination. The star positions are taken from a

catalog and refer to its epoch. Precession and nutation are therefore applied to refer
the observation to the reference system desired. For reasons related to the orbital
theory for r(t), we have chosen to work in the quasi-inertial reference system defined
by the equinox of 1950.0 and the equator of date. In addition, UT1 and pole positions
are applied to bring the terrestrial reference frame, defined by the Conventional
International Origin and the zero meridian of the BIH, into this system. Therefore,
orbital elements and station positions are expressed in this quasi-inertial reference
system when determined with direction observations. Specifically, the right ascension
of the ascending node of the satellite (hereafter called the node) is unambiguously
defined.

Observations of range relate the relative position of the satellite to the observer
and not to the reference system; i.e., the observation is unchanged if the reference
system is transformed by translation or rotation. Specifically, the node is defined
only relative to the adopted value of ÷UT1. Therefore, when only observations of
range (and velocity) are used to determine coordinates, a correction for the longitude
must be allowed for in each orbit.

Optical data were assigned an assumed accuracy of 4". In those instances in
which five or more observations were made within a few minutes — e.g., of Geos
flashes — a smoothed or synthetic observation was determined. The same calculation
was used to generate simultaneous observations, because one cannot, in general, make
exactly simultaneous observations. These synthetic observations were assigned an
accuracy determined from the polynomial fit. If the computed uncertainty was less
than 2", then 2" was used. Laser data have a precision of 1 to 2 m in distance meas-
urements; however, timing errors and other errors such as those due to the gravity
field must be taken into account. Therefore, we have used the assumed accuracies
listed in Table 9.

The data were kept in two parts. Before 1970, most of the observations were direc-
tions. A number of laser ranges were made, and where it was possible to do so,
they were included in the orbits. In 1971, the cooperative tracking program ISAGEX,
with 10 laser stations, provided for the first time relatively complete orbital and
geographical coverage with laser data. From these ISAGEX data, 15 orbits were used

in the dynamical determination of station coordinates. Table 10 gives the number of observations selected both from pre-ISAGEX data and from ISAGEX data. The dynamical solution was based on 140 arcs of 15 satellites from the pre-ISAGEX data taken between 1962 and 1969, and 15 arcs of 3 satellites from the ISAGEX data taken in 1970. Since ISAGEX data are of a new type, we examined the origin of the node and the relative weighting in order to find the best treatment. The pre-ISAGEX data were in arcs of from 4 to 30 days long, as appropriate, and the ISAGEX data were in 10-day arcs.

For all practical purposes, the length scale in a dynamical solution is fixed by the value of GM, which directly enters the calculations of the radius vector through

$$r = \left(\frac{GM}{n}\right)^{1/3} (1 \div e \cos E)(1 \div \text{perturbations}) \quad .$$

With optical directions, no further information in scale is available. With range data, both scale and GM can, in principle, be determined. The unit of distance is then defined by the speed of light and becomes the "light second." In this analysis, GM was assumed to have the value given in Table 11, and our dynamical scale is therefore defined by GM. If this value of GM is far from the exact one, some deterioration of the coordinates will occur. We will return to this question in Section 3.4.

3.3 Combination Solution for Coordinates

The six sources of data combined are the following:

SAO dynamical network (pre-ISAGEX),
SAO dynamical network (ISAGEX),
SAO geometrical network,
BC-4 geometrical network,
JPL dynamical network (DSN),
Geodetic coordinates.

As described above, each subset of data was processed individually, with certain internal checks being allowed. Each subset was reduced with its own a priori weighting scheme, which was internally consistent. The greatest difficulty in combining these

six sets of data was to establish realistic relative weights for each system. Relative weighting is derived by experiment tempered with some notion of the accuracy and by comparison with datum coordinates and heights. Only the SAO dynamical network and certain geodetic coordinates could not be taken at their given weight.

The geodetic coordinates provided the greatest source of concern and uncertainty in the analysis. Except for the SAO networks, the geodetic coordinates provide the only link between networks, and within networks, the link between collocated stations (e.g., 4761-4762, 6111-6134). Geodetic coordinates were used as observations between relatively close stations — i.e., separated by less than 100 km — because the accuracy may not be so good for greater distances and because the use of geodetic coordinates as described above assumes no datum tilt nor scale difference.

Each subset of data was treated to provide a system of normal equations and normal residuals. The systems are combined with their relative weights. In addition, each system may have a different origin, orientation, and scale, but these differences should not occur if each system had been referred to the defined system without error. In the combination, additional parameters as necessary were introduced into the combined normal system to account for possible systematic errors. The SAO dynamical pre-ISAGEX data were taken as the reference. Since the geometrical networks have no scale, only translation and rotation parameters were introduced. For practical purposes, the SAO geometrical network covers only one hemisphere in an east-west orientation, so only the rotation about the z axis (ϵ_z) may be meaningful. This corresponds to a correction to UT1. The polar orientation for the SAO geometrical network (ϵ_x, ϵ_y) turned out to be smaller than the formal uncertainty. The JPL net had only a scale and ϵ_z parameter as it is not sensitive to ϵ_x, ϵ_y or to the origin. Experiments with determining corrections to the node ($\Delta\Omega$) for each arc of ISAGEX data indicated that 1) the corrections were small, generally less than 1 μrad, and 2) they were satisfactorily included through the reduced normal equations. Therefore, formally, the combination solution contained 14 additional parameters, the final values of which are given in Table 12. The translation of the two geometrical networks is the correction to the station used as the origin. Excellent agreement occurs between these translations and the coordinates determined from an a posteriori geometric adjustment. The formal uncertainty for the translation of the SAO geometrical network is not given, because the origin station 9051 has very few observations and is not determined very well.

Two iterations were completed; the first starting with the coordinates given in Gaposchkin and Lambeck (1970). Examination of the solutions indicated problem stations; in particular, the geodetic coordinates were sometimes seriously in error. The strategy used to determine the relative weights and the formal uncertainty was based on the geometrical solutions, and all other solutions were referred to them.

The accuracy of each station-to-station direction was computed. This estimate can be verified by comparison with the direction determined in the network adjustment. The adjustment essentially enforces the coplanarity condition for any three directions that connect three stations. By comparing these estimates of the direction, we can compute a scale factor that is a measure of the agreement between the formal statistics of the adjustment and the actual errors. This scale factor turned out to be $k^2 = 2.65$ for the SAO geometrical network and $k^2 = 2.60$ for the BC-4. Since the difference between these estimates of k^2 is not significant, we adopted an overall scale factor of $k^2 = 2.625$ for the geometrical networks. It is interesting to note that when only the 12 SAO Baker-Nunn cameras are used, the scale factor becomes $k^2 = 1.03$, indicating excellent control of systematic errors.

In the combination of the six types of data, the geometrical networks, the JPL network, and the geodetic survey data were used with a priori variances. The pre-ISAGEX dynamical data were given a weight of 0.25 for the combination of the normal equations, which effectively doubles the assumed accuracy. In addition, the assumed accuracy of the pre-ISAGEX laser data was further multiplied by a factor of $1/\sqrt{10}$, and thus the assumed accuracy of the laser data was multiplied by 6. The ISAGEX data were given an overall weight of 0.0625; i.e., the assumed accuracy was multiplied by 4. Thus, the reference orbits were computed by using the assumed accuracy in Table 9, but the normal system was scaled by these factors. These adjustments were necessary in order to accommodate the enormous volume of data used for the dynamical solutions. Large volumes of well-distributed data lead to cancellation of random errors, which is desirable, but give optimistic estimates of variance. The balance of weights presented here leads to an internally consistent solution, which has acceptable agreement with independent data. Table 13 lists the geocentric coordinates for the stations determined in SE III, together with their uncertainties scaled by $k^2 = 2.625$.

3.4 Comparisons

The combination solution for coordinates scaled by $k^2 = 2.625$ gave estimates of variance of 2 m for the best stations. Since no comparison exists that can verify this accuracy for geocentric coordinates, we are limited to consistency checks. The coordinates should agree with the standard at least as well as the accuracy of the standard. A number of internal checks (e.g., between geometrical and dynamical solutions) can be performed. Comparisons can be made with surface data, but they test only the relative position and not the geocentric position of the coordinates. Nevertheless, these comparisons are instructive and indicate that the computed variances (uncertainties) are realistic estimates. Further, the general agreement internally in the satellite data -- and externally with the terrestrial data -- indicates that, as a rule, discrepancies are within the expected uncertainties. The large discrepancies are probably due to errors in the survey data, and further analysis is needed.

Comparisons with satellite orbits are inconclusive at best, because of the large number of error sources. In Section 4.4, numerical results are given for orbit computations with laser data by using the latest gravity field and station coordinates. This comparison indicates that the orbit computing system (data, theory, physical parameters, and station coordinates) has an accuracy of 5 to 10 m, which is not inconsistent with a 2- to 5-m accuracy for the station coordinates.

The typical direction is determined with an accuracy of 5 μrad, equivalent to a relative position of 10 m. For selected sets of stations, Figure 6 compares the determined direction (both before and after the coplanarity condition is applied), the dynamical solution, and the combination solution. In some cases, a direction from the SAO geometrical net and another from the BC-4 geometrical net are available. These comparisons are perhaps unfavorable in that the errors of both stations are reflected in the figures. The error ellipses for all the directions are scaled by the factor $k^2 = 2.625$. In order to express all the directions in the same coordinate system, the plotted directions are rotated by the parameters given in Table 12.

When the origin and scale are provided, the BC-4 network of 48 stations gives a geometric solution that can be compared with the combination solution. Table 14 gives the results of such a comparison, with residuals in X, Y, and Z and north, east, and height. The geometrical solution has an average uncertainty of 5 m for each coordinate, while the combined solution has the uncertainty given in Table 13. The adjustment uses a weight computed from the two solutions. The rms of 12 m and the standard error of unit weight $\sigma_0 = 0.8$ indicate the excellent agreement in the coordinates and the estimated uncertainties. A number of individual coordinates are too large. The north-south residual of -25 m for station 6068, which is tied geodetically to 7902 and 4751, is the most troublesome.

The JPL coordinates given by the LS 37 solutions, rotated and scaled by the results in Table 12, are compared in Table 15 with the coordinates determined in the combination solution.

Comparisons within each datum are possible. The four major datums where this was done are as follows:

> North American datum (NA27),
> South American datum (SA69),
> Australian datum (AUGD),
> European datum (EU50).

As described earlier, the use of datum coordinates in the combination solution has been restricted to nearby stations, primarily in order to relate different types of observations. Therefore, datum coordinates constitute a relatively independent set of data. However, each datum has an arbitrary origin, orientation, and scale, and the relation between each datum and the geocentric system must be determined. One can therefore determine up to seven parameters, but depending on the size of the datum and the distribution of stations on the datum, some of these transformation parameters may not be significant. The seven transformation parameters are three translations, three rotations, and one scale. We have elected to express the rotations as rotations of the datum origin about the normal to the ellipsoid and around two axes in the tangent plane

oriented north–south and east–west. These rotations have a physical interpretation since they express an error in the azimuth of orientation of the datum and a tilt of the datum ellipsoid. Accordingly, the transformation will be given by

$$\overline{X}_{sat} = \overline{X}_{dat} + \overline{T} + (1 + K)\ \overline{\overline{R}}\ (\overline{X}_{dat} - \overline{X}_0)\ \ ,$$

where $\overline{X}_{sat}$ and $\overline{X}_{dat}$ are the coordinates from the satellite solution and the datum, respectively, $\overline{T}$ is the vector of the three translation parameters, K is the scale correction, $\overline{X}_0$ are the coordinates of the datum origin, and $\overline{\overline{R}}$ is a rotation matrix dependent on the three rotational parameters and the latitude and longitude of the datum origin.

Table 16 gives the translation, rotation, and scale parameters for four major datums as computed from the adjustment of the datum coordinates to the satellite solution. A positive scale here means that the datum scale has to be increased in order to agree with the satellite scale. The table also gives the number of stations used in each datum. In the computation of datum shifts, each station was assigned a weight computed from the standard deviation of the satellite solution and the standard deviation of the datum coordinates, which was taken as $\sigma = 5 \times (S \times 10^{-6})^{2/3}$ (m), where S is the distance of the station from the datum origin in meters. In all cases, the standard deviation of unit weight σ_0 (given in Table 16) after the adjustment is smaller than 1, which means that the weights are somewhat pessimistic. The rms σ (m) of the final residuals for each datum in Table 16 are between 5 and 16 m. It is apparent that the European and the South American datum coordinates do not agree very well with the satellite solution. The European datum is rather unhomogeneous, and its extension into Africa and Asia — which we used — makes it rather weak.

Further checks with datum information can be obtained with station heights. The height above the reference ellipsoid (h_{ell}) should be equal to the mean height above sea level (h_{msl}), which is approximately the height above the geoid, plus the geoid height N; i.e., the disagreement between these two estimates, Δh, is

$$\Delta h = h_{ell} - h_{msl} - N\ \ .$$

If we use the satellite geoid to calculate N, we can make this comparison for all stations but we lose the detailed variation in geoid height. The computation does provide a value for the semimajor axis of the best-fitting ellipsoid used to calculate h_{ell}. We get

$$a_e = 6378140.4 \pm 1.2 \text{ m} \quad .$$

To employ the detailed geoid-height information given for each datum, we must refer the coordinates to the datum origin by using the datum shifts in Table 16. Table 17 lists the standard deviations of the heights calculated for each datum. The average of 3.98 m must be considered excellent in view of all the uncertainties in calculating Δh. Figure 7 plots these residual heights as a function of latitude.

The results by Gaposchkin and Lambeck (1970) were derived in the same manner, by combining several types of data, establishing relative weights, and verifying the accuracy by intercomparison. Their accuracy was 7 to 10 m for the fundamental stations. In Table 18, we give the corrections derived in this analysis for selected stations. The overall rms of $\sigma = 10$ m and a standard error of unit weight $\sigma_0 = 0.662$ indicate excellent agreement in the derived coordinates and the accuracy estimates; if anything, the accuracy estimates are pessimistic. The very small shift in origin indicates that the whole reference system has not changed.

Williams, Mulholland, and Bender (1972) have determined the spin-axis distance of McDonald Observatory from lunar laser observations. We compare this distance with that deduced by means of the coordinates of station 9001 from survey data in the following. The agreement of -3.51 m is acceptable.

Using SAO station 9001 and geodetic tie	5492412.489 m
Using McDonald lunar laser	5492416.0 $\pm$ 3 m
Difference	-3.51 m

The scale of the combination solution is defined by the value of GM adopted in the dynamical solution, given in Table 11. We found a scale difference of 0.18 $\pm$ 0.55 ppm between the JPL and the SAO coordinates, the JPL ones being slightly larger. If the discrepancy with the lunar laser is attributed to scale, then the scale difference would be 0.7 ppm.

The scale obtained from the four major datums is given in Table 16. It appears from the NA27, EU50, and AUGD datums that the datum scale is smaller than the satellite scale by approximately 2 ± 1 ppm, while from the SA69 datum, it is larger by 1 ± 1 ppm. Since the survey scales are not expected to be established to better than a few ppm, the weighted mean of 1.6 ± 1 ppm is not considered to be significantly different from zero.

Each geometrical network has an arbitrary origin specified by the initial coordinates of one station, a station not explicitly determined in the combination solution. The translation parameters in Table 12 correspond to the correction to the origin of the network, i.e., the correction to the initial coordinates of the reference station.

In principle, the orientation of the two geometrical systems and that of the dynamical system should be identical. Orientation parameters $(\epsilon_x, \epsilon_y, \epsilon_z)$ are determined to accommodate possible systematic differences in the actual representation of the three systems. Since the SAO geometrical network covers only one hemisphere in an east-west orientation, the orientation of its pole (ϵ_x, ϵ_y) may be poorly determined.

The polar orientation of the BC-4 system with respect to the SAO dynamical system is $1.88 = \sqrt{1.76^2 + 0.65^2} \pm 1.16$ μrad. This systematic difference is obtained by comparing the observed BC-4 directions with directions determined from 11 stations in the combination solution with characteristic interstation distances of 2 to 3 Mm. In metric terms, the orientation difference is $1.88 \times 10^{-6} \times 2 \times 10^{6} \approx 4$ m. The accuracy of the mean station for the 11 stations is approximately 4 m. It is assumed that the value of 1.88 μrad results from differences in pole-position data or in processing methods.

The rotation in longitude (ϵ_z) corresponds to a correction in UT1. Figure 8 indicates the relative position of the zero meridian of each system. We note almost the same relation between the SAO and the JPL systems found in SE II, which was 4.0 μrad. The difference between the SAO geometrical and the SAO dynamical systems is -0.40 ± 1.43, and that between BC-4 and the SAO dynamical is -2.20 ± 0.82. The

relative rotation in longitude between the JPL and the SAO systems is due to a difference between the JPL's planetary ephemeris and the FK4 system used by SAO. The JPL ephemeris is referred to the dynamical equinox rather than to the FK4 system (D. Trask and T. C. Van Flandern, private communication, 1974). The difference 0."7 is almost exactly equal to the 3.43 ± 1.02 μrad determined in this analysis. The longitude difference between the geometrical and the dynamical nets most likely results from differences in the UT1 data or in the processing methods.

4. DETERMINATION OF THE GEOPOTENTIAL

4.1 Methods

The external potential of the earth is represented by a set of orthogonal functions:

$$U = \mathcal{R}e \frac{GM}{r} \sum_{\ell=0}^{\infty} \sum_{m=0}^{\ell} \left(\frac{a_e}{r}\right)^{\ell} \overline{C}_{\ell m} \, \overline{P}_{\ell m}(\sin\phi) \, e^{im\lambda} \quad , \tag{3}$$

where M is the mass of the earth, including the atmosphere; G is the universal constant of gravity; $\overline{C}_{\ell m} = \overline{C}_{\ell m} - i\overline{S}_{\ell m}$; $\overline{C}_{\ell 0} = -J_{\ell}/\sqrt{2\ell+1}$; $\mathcal{R}e\{\ \}$ designates the real part of $\{\ \}$; $\overline{P}_{\ell m}(\sin\phi)$ are fully normalized associated Legendre polynomials; and r, ϕ, λ are the coordinates of the test particle. It is possible to choose a coordinate system such that

$$\overline{C}_{1,0} = \overline{C}_{1,1} = \overline{C}_{2,1} = 0 \div i\,0 \quad ,$$

and we assume that the instantaneous spin axis as defined by IPMS and the center of gravity of the earth are that system. This assumption is not strictly true, but the departures are small and are ignored in this analysis.

It is observed that for the earth the amplitude of $E\left(|\overline{C}_{\ell m}|\right)$ decreases approximately according to

$$E\left(|\overline{C}_{\ell m}|\right) = \frac{10^5}{\ell^2} \quad . \tag{4}$$

Although for theoretical reasons $E\left(|\overline{C}_{\ell m}|\right)$ must decrease more rapidly than equation (4) at some point, and individual coefficients can be arbitrarily large, this rule seems valid throughout the range of ℓ used in this investigation.

.We use two types of data on the earth's gravity field: those derived from gra-
vimeters and those obtained from the motion of artificial satellites. The gravity
calculated from the gradient of equation (3) is

$$\Delta g = \gamma \, \mathcal{Re} \sum_{\ell=2}^{\infty} \sum_{m=0}^{\ell} (\ell-1) \left(\frac{a_e}{r}\right)^{\ell} \overline{\mathcal{C}}'_{\ell m} \, \overline{P}_{\ell m}(\sin\phi) \, e^{im\lambda} \quad , \tag{5}$$

where $\gamma = GM/r^2$ and $\overline{\mathcal{C}}'_{\ell m}$ are $\overline{\mathcal{C}}_{\ell m}$ modified to accommodate those effects of the
reference ellipsoid (or gravity formula) that change the definition of $\overline{\mathcal{C}}_{2,0}$, $\overline{\mathcal{C}}_{4,0}$,
and $\overline{\mathcal{C}}_{6,0}$. By comparing equations (3) and (5), it is apparent that Δg is relatively
more influenced by $\overline{\mathcal{C}}_{\ell m}$ of high degree and order than is $\mathcal{U}$ because of the $\ell - 1$
multiplier and that measurements of Δg are more useful for determining these high-
degree and high-order coefficients.

Determination of $\overline{\mathcal{C}}_{\ell m}$ from analysis of satellite observations requires a theory
for satellite motion. General solutions for the motion in an arbitrary potential field
have not yet been found. We must therefore restrict ourselves to approximate solu-
tions, which are quite sufficient for the following reasons. It is observed that for the
earth, the second-degree zonal harmonic $\overline{\mathcal{C}}_{2,0}$ makes the largest contribution to the
anomalous potential and is 10^{-3} of the main term. The remaining anomalous potential
is 10^{-3} of $\overline{\mathcal{C}}_{2,0}$, or 10^{-6} of the main term. Therefore, to calculate the trajectory
to 10^{-6} (our objective), we require at least a second-order theory for $\overline{\mathcal{C}}_{2,0}$ (i.e.,
one including $\overline{\mathcal{C}}_{2,0}^2$), but only a first-order linear theory for the remaining $\overline{\mathcal{C}}_{\ell m}$.
Although there are notable exceptions — resonances and some zonal harmonics — these
considerations provide a workable base.

The earth's motion is complicated because of precession, nutation, polar motion,
and rotation. A convenient reference frame is defined by the stars and, in practice,
is defined (imperfectly) in terms of a star catalog at some epoch. On the other hand,
in an inertial frame, the earth's gravity field has a temporal variation that significantly
complicates the construction of an analytical theory. For this reason, a compromise
quasi-inertial reference frame referred to an equinox (epoch 1950.0) and an equator
(epoch of date) has been adopted. Veis (1960) knew, Kozai (1960) proved, and we have
used the fact that this coordinate system minimizes the additional effects required to
account for the temporal variations of the gravity field and the noninertial property of
the coordinate system.

Accordingly, the determination of $\overline{C}_{\ell m}$ from analysis of satellite observations uses the elaboration of a satellite-perturbation theory. This elaboration is too lengthy to detail here; we refer the reader to Gaposchkin (1973).

In summary, the process of gravity-field determination begins with the evaluation of the secular and long-period perturbations to determine the J_n. The perturbations accumulate for weeks and months, and the effects are very large. The mean orbital elements, determined from overlapping 4-day arcs, constitute the basic data used in the analysis. Data and reference orbits of moderate accuracy are adequate for the J_n determination. The unbiased recovery of the J_n requires painstaking evaluation of the long-period and secular perturbations from other sources, principally solar radiation pressure, atmospheric drag, and lunar and solar attraction. This phase of the analysis is accomplished first. The tesseral harmonics are determined from the short-period (1-revolution to 1-day) changes in the orbit. The detailed structure of the orbit must be observed, and each observation provides an observation equation. Data of the highest possible precision are needed. The unbiased recovery of $\overline{C}_{\ell m}$ requires the evaluation of the periodic terms from other sources that have periods similar to those arising from the gravity-field coefficients. The most important are the short-period terms due to J_n and the lunar attraction. Because they are smaller than 1 m for the satellites used in this analysis, the periodic effects of air drag and radiation pressure can be ignored. The nonperiodic terms are empirically determined and hence accounted for. The short-period terms due to J_2 must be carried to second order.

4.2 Coefficients of Zonal Spherical Harmonics in the Geopotential

Coefficients of zonal spherical harmonics in the geopotential determined from secular motions of angular variables and from amplitudes of long-periodic terms with the argument of perigee ω in the orbits of artificial satellites are more accurate than are coefficients derived by classical terrestrial methods. The reason is that the component of geoid height represented by the zonal harmonics is amplified by a factor of 1000 when they appear as secular and long-periodic perturbations of satellites. However, because these perturbations are averaged effects, contributions from the harmonics in each are not very different from one satellite to another unless their orbital elements are quite different. Also, few satellites with inclinations below 30° have been

employed in the determination of the coefficients, since accurate observations of such satellites have been scarce. It was also found that many more terms than expected were necessary to represent the geopotential. Therefore, it has usually been very difficult to separate the contributions from each harmonic in the observed values of the secular motions and of the amplitudes of the long-periodic terms. In other words, different sets of coefficients could represent these observations within observed accuracies for satellites with inclinations larger than 30°.

Now, however, data for two low-inclination satellites – Dial (7001701; I = 5°4, e = 0.09, a = 1.15) and Peole (7010901; I = 15°0, e = 0.02, a = 1.10) – have become available since our last determination of zonal harmonics (Kozai, 1969).

The equations of condition were solved by least squares for both the even-order and the odd-order harmonics. They were solved first with 11 unknowns, J_n (n ≤ 23), and then with 12, the twelfth being J_n (24 ≤ n ≤ 49). Seven solutions were obtained. The solutions are quite stable, especially for lower order coefficients, and the observations can be represented very well by including J_{35} and J_{36}. Although there is some uncertainty whether J_{35} and J_{36} can have such large values, the 12-unknown solutions that include them are regarded as the best. For further details, see Gaposchkin (1973). The adopted numerical values of the zonal harmonics are given in Table 19.

4.3 Determination of Tesseral Harmonics

Tesseral harmonics are computed by combining satellite perturbations and terrestrial gravimetry. In the computation of the normal system, terms with small contributions have been omitted. Therefore, the normal system determined from satellite analysis is complete through $\ell = m = 12$. In each higher order, terms have been omitted – for example, 13, 6 through 13, 9 and 14, 5 through 14, 11. The higher order terms selected were C/S(ℓ, 1) 13 ≤ ℓ ≤ 16; C/S(ℓ, 2) 13 ≤ ℓ ≤ 15; C/S(14, 3); C/S(ℓ, 12) 13 ≤ ℓ ≤ 19; C/S(ℓ, 13) 13 ≤ ℓ ≤ 2; and C/S(ℓ, 14) 14 ≤ ℓ ≤ 24. Of course, all terms were included in the computation of the residuals. In the same way, for surface gravity all available geopotential coefficients have been used, but no partial derivatives for the zonal harmonics or tesseral harmonics less than 9th degree were computed, since they are negligibly small.

For each orbital arc, a set of six mean elements, $\mathcal{E}_i$, is determined. The linear rates are derived empirically, as is the mean anomaly. In addition, higher polynomials in the mean anomaly are employed, where appropriate, to account for the nonperiodic, yet nonsecular, effects of air drag and radiation pressure. Twelve or more orbital elements are determined for each arc, and the arcs range in length from 4 to 30 days.

The m = 9, 12, 13, 14 terms are resonant with some satellites, which are listed in Table 20 along with their resonant periods. Several satellites are resonant with more than one order.

A summary of the data is given in Table 1. The selection of data and unknowns evolved through the analysis. The number of satellites used ranged from 21 to 25, and the number of arcs in the largest solution was 203. Arcs were added or rejected on the basis of their contribution to the normal equations, the number of observations for a particular station, the improvement of distribution for a resonant harmonic, and the quality of the orbital fit.

Two iterations were performed for the gravity field. The first employed the gravity field and station coordinates determined by Gaposchkin and Lambeck (1970) as initial values; and the second used the results of the first iteration for the gravity field plus the station coordinates as described earlier. For each iteration, several solutions were obtained. Orbital arcs were added or deleted to improve the satellite distribution and the variance-covariance matrix.

Several weights for the surface gravity were used. For areas without surface-gravity data, we had four choices of treatment:

A. We could make no assumptions about unobserved areas.

B. We could use a zero anomaly with a very large variance; that is, the expected value of gravity would be zero.

C. We could use a reference gravity field with a very large variance; that is, only the higher harmonics would have an expected value of zero.

D. We could use a model anomaly, for example, one determined from topography.

Adoption of method A would introduce very large short-wavelength features into those regions where no gravity is measured. In addition, the statistical comparisons discussed later are very poor, although the (O – C) values and the satellite orbits are good. Therefore, A had to be discarded. Gaposchkin and Lambeck tried methods B and D and found them equivalent. Choice C is an improvement over B because the low-degree and low-order terms are well determined by means of satellite data. Therefore, C was adopted, with the weight given in Table 21. Comparing the results of choices A and C, we found that satellite comparisons are identical, the (O – C) for the surface gravity is marginally improved, and the statistical comparisons of the surface gravity are quite acceptable. The adopted accuracy of a gravity anomaly with one observation was determined by experiment. The optimum combination solution used 13.5 mgal, in acceptable agreement with 17.7 mgal obtained from the variance in Table 8.

The fully normalized spherical-harmonic coefficients for the tesseral harmonics are given in Table 22. Figure 9 shows the mean potential coefficient by degree and the $10^{-5}/\ell^2$ rule. The mean potential coefficient for degrees 2 through 36 is determined by numerical quadrature of surface-gravity data and is also plotted in Figure 9. Figure 10 plots the geoid heights and gravity anomalies: Figures 10a and 10b are calculated from the coefficients in Tables 19 and 22 with respect to the best-fitting ellipsoid; Figures 10c and 10d, with respect to the hydrostatic ellipsoid; and Figures 10e and 10f, with respect to the 5th-degree and order reference surface defined by the 5th-degree and order coefficients from Tables 19 and 22.

4.4 Evaluation of Geopotential

A detailed evaluation of SE III results with satellite orbits is difficult. Although other effects — such as lunar and solar perturbations, body tides, radiation pressure, and air drag — are all included in the orbit computation, none of these is known without error, and each, in itself, provides a number of problems. Also, the coordinates of the tracking stations are not known without error. Furthermore, incomplete orbital coverage can result in overoptimistic estimates of orbital accuracy from formal statistics. Finally, the tracking data contain errors. A few comparisons are given here to indicate approximately the accuracy of the total orbit-computation system. The gravity field is certainly one of the larger contributors to the error budget.

From ISAGEX data, consecutive orbits were computed every 2 days, by using 4 days of data (except for 6800201, where 6 days of data were employed). Results for 6508901, 6800201, and 6701401 are given in Table 23, together with the number of observed points used in the final iteration. All calculations were performed by using the final station coordinates and the tidal parameter $k_2 = 0.30$; radiation-pressure perturbations were calculated with a fixed area-to-mass ratio.

We see that with good orbital coverage, we can expect to have rms residuals of between 4 and 10 m. Satellite 6701401 has a relatively low perigee, and the poorer orbits from MJD 41072 to 41078 coincide with an increase in solar activity that resulted in increased drag.

Of the 4- to 10-m rms residuals, 2 to 3 m come from station coordinates and 1 to 4 m could be attributed to the orbital theory. Therefore, the accuracy of the gravity field for orbit computation may actually be somewhat better than indicated by Table 23.

To compare a geopotential model (g_s) with observed values of surface gravity (g_t), the following quantities defined by Kaula (1966) can be computed:

$\langle g_t^2 \rangle$ — The mean value of g_t^2, where g_t is the mean free-air gravity anomaly based on surface gravity, indicating the amount of information contained in the surface-gravity anomalies.

$\langle g_s^2 \rangle$ — The mean value of g_s^2, where g_s is the mean free-air gravity anomaly computed from the geopotential model, indicating the amount of information in the computed gravity anomalies.

$\langle g_t g_s \rangle$ — An estimate of g_h — i.e., the true value of the contribution to the gravity anomaly of the geopotential model and the amount of information common to both g_t and g_s.

$\langle (g_t - g_s)^2 \rangle$ — The mean-square difference of g_t and g_s.

$E(\epsilon_s^2)$ — The mean-square error in the geopotential model.

$E\left(\epsilon_t^2\right)$ The mean-square error of the observed gravity.

$E\left(\delta g^2\right)$ The mean square of the error of omission — that is, the difference between true gravity and g_h; this term is then the model error.

If the geopotential model were perfect, then $\langle g_s^2 \rangle = \langle g_h^2 \rangle$, which in turn would equal $\langle g_t g_s \rangle$ if g_t were free from error and known everywhere. Then, ϵ_s^2 would be zero even though g_s would not contain all the information necessary to describe the total field. The information not contained in the model field — i.e., the error of omission, δg — then consists of the higher order coefficients. The quantity $\langle (g_t - g_s)^2 \rangle$ is a measure of the agreement between the two estimates g_t and g_s and is equal to

$$\langle (g_t - g_s)^2 \rangle = E(\epsilon_s^2) + E(\epsilon_t^2) + E(\delta g^2) \quad .$$

Another estimate of g_h can be obtained from the gravimetric estimates of degree variance σ_ℓ^2 (Kaula, 1966):

$$E(g_h^2) = D = \sum_\ell \frac{n_\ell}{2\ell + 1} \sigma_\ell^2 \quad ,$$

where n_ℓ is the number of coefficients of degree ℓ included in g_h, and

$$\sigma_\ell^2 = \gamma^2 (\ell - 1)^2 \sum_m \left(\overline{C}_{\ell m}^2 + \overline{S}_{\ell m}^2 \right) \quad .$$

We also have

$$E(\epsilon_s^2) = \langle g_s^2 \rangle - \langle g_s g_t \rangle$$

and

$$E(\epsilon_t^2) = \langle g_t^2 \rangle / \langle n \rangle \quad .$$

. Table 24 summarizes the above quantities for SE III. The improvement over SE II in the coverage of surface-gravity data is evident. The more limited gravity coverage used for SE II resulted in accuracy estimates that were consistently optimistic. The revised set of gravity anomalies has greater coverage and is more independent of the geopotential model. Even so, line 2 represents an estimate of the accuracy, $E(\epsilon_s^2) = 52$ mgal^2, that is more optimistic than that based on independent gravity data for SE II, which was 99 mgal^2 (Gaposchkin and Lambeck, 1970).

We used the 306 gravity anomalies with 20 or more observed units in each average for the comparison. There is very good agreement between $\langle g_t g_s \rangle$, $\langle g_s^2 \rangle$, and D, which would all be equal for a perfect solution. In $E(\delta g^2)$, we have a measure of the information remaining in the higher harmonics. The formal statistics give an error in the combination reference field of $E(\epsilon_s^2) = 15$ mgal^2.

An alternative approach is to eliminate δg by use of

$$\begin{bmatrix} \Delta \overline{C}_{\ell m} \\ \Delta \overline{S}_{\ell m} \end{bmatrix} = \frac{1}{4\pi\gamma(\ell-1)} \int_{\text{sphere}} (g_t - g_{\text{ref}}) \left\langle \overline{P}_{\ell m}(\sin\phi) \begin{bmatrix} \cos m\lambda \\ \sin m\lambda \end{bmatrix} \right\rangle d\sigma \quad,$$

where

$$\left\langle \overline{P}_{\ell m}(\sin\phi) \begin{bmatrix} \cos m\lambda \\ \sin m\lambda \end{bmatrix} \right\rangle \quad \text{is the mean of} \quad \overline{P}_{\ell m}(\sin\phi) \begin{bmatrix} \cos m\lambda \\ \sin m\lambda \end{bmatrix}$$

over the area defined for the gravity anomaly. We can compute any harmonic with respect to a reference gravity field, but care must be used in treating areas where no observed gravity is available. A gravity field defined by g_{ref} and the $\Delta\overline{C}_{\ell m}$, $\Delta\overline{S}_{\ell m}$ will have an error of

$$\langle (g_t - g)^2 \rangle = E(\epsilon_s^2) + E(\epsilon_t^2) + E(\delta g^2) + E(\epsilon_{\text{quad}}^2) \quad,$$

where $E(\epsilon_s^2)$ is the error in the composite field and $E(\epsilon_{\text{quad}}^2)$ is the error due to the inexact quadrature and imperfect distribution of the data.

Table 25 gives the results of this numerical quadrature with reference fields defined by the first ℓ degrees of SE III. Computing all the geopotential coefficients to $\ell = m = 36$, i.e., the null reference field, we get $E(\epsilon_s^2) \equiv 0$, and

$$E(\epsilon_t^2) + E(\delta g^2) + E(\epsilon_{quad}^2) = 29 \text{ mgal}^2 \quad .$$

Using an increasingly detailed reference field, we obtain an estimate of $E(\epsilon_s^2)$ as a function of degree. As expected, the mean-square error for the low-degree and low-order harmonics estimated from a comparison with terrestrial gravimetry is quite small. The satellite data provide accurate values, and the low harmonics have a smaller effect on gravity anomalies. The mean-square error for the 8th to 18th degrees is relatively constant, as expected, since these harmonics are determined largely by surface-gravity data. The mean-square error $E(\epsilon_s^2)$ estimated from the quadrature is in good agreement with that obtained from statistical analysis. For comparison, the values are given in Table 24.

The estimate of $E(\epsilon_s^2)$ assumes that g_s and g_t are independent; i.e., they have uncorrelated errors. Since the terrestrial gravity (g_t) was used to determine the combination solution (g_s), this assumption is certainly incorrect, and therefore, the estimate of $E(\epsilon_s^2) = 15 \text{ mgal}^2$ is definitely optimistic. A better test could be made·with independent data for g_t. Since the mean gravity anomalies used in the combination solution were computed, two compilations of $1° \times 1°$ anomalies have been published: for North America and the North Atlantic (Talwani, Poppe, and Rabinowitz, 1972) and for the Indian Ocean (Kahle and Talwani, 1973). These compilations were published after the set of mean anomalies used here became available, but some basic data are probably common to both; furthermore, these two new compilations may not be completely independent of the data used in the SAO combination solution. The processing methods used by Talwani and his coworkers were different from those of ACIC, and additional data were included.

Two comparisons are nevertheless instructive. A simple $5° \times 5°$ average was computed for these data since all $1° \times 1°$ areas had values given in the region of interest. These $5° \times 5°$ averages, with the mean of the whole region subtracted, were

used to compute the same statistical quantities as in Table 24 and are given in Table 26. The number n is the number of points, centered in a $1° \times 1°$ area, for which a $5° \times 5°$ mean was computed. Therefore, we have a moving $5° \times 5°$ mean calculated every $1°$. Most of the gravity data in these ancillary compilations were taken at sea, and the estimate of their uncertainty $E(\epsilon_t^2)$ may be optimistic. The weighted mean of $E(\epsilon_s^2)$ is 64 mgal^2, equivalent to 2.5 m in geoid height. The remaining gravity information in the higher harmonics, δg, equals 68 mgal^2. We notice that δg for the Indian Ocean is larger than δg for North America and the Atlantic and is probably due to the very sharp low below the Indian subcontinent, which cannot be modeled very well by the generalized geoid. Further confidence in this comparison comes from $\langle (g_t - g_s)^2 \rangle$, $\langle g_s^2 \rangle$, $\langle g_t^2 \rangle$, and $\langle g_t g_s \rangle$, which are all in good agreement with the global values from Table 24. Therefore, we feel reasonably certain that for comparison purposes, both the North America and North Atlantic region and the Indian Ocean region are typical. Thus, we conclude that the generalized geoid has an accuracy of ±2.5 in geoid height and ±8 mgal for the whole earth. Figures 11 to 15 give north–south and east–west profiles for both North America and the Indian Ocean.

Figure 15 was selected because of the large change in the values at the India Low from those given in SE II. However, the terrestrial gravity and the combination solution are in good agreement there. A further point is the disagreement, east of Borneo, between the observed gravity from the ACIC compilation and the anomalies used in 1969.

5. SUMMARY AND CONCLUSIONS

The results described above, the procedures, the tests and comparisons, and the experience of carrying out the work have led to several conclusions about the use of artificial satellites for the determination of station coordinates and the geopotential:

A. Observations of close-earth satellites have been successfully combined with observations of deep-space probes and surface triangulation, enabling us to determine the coordinates of 90 satellite-tracking sites in a uniform homogeneous system.

B. The combination of these data provides a better solution than we can obtain from each set of data separately, because more complete coverage results and because the combination enables us to overcome weaknesses in each system.

C. The methods of processing each type of data are sufficiently understood to make a rational combination.

D. Successive solutions have resulted in improvements. When compared with the previous solution, each new one has agreed to within the estimated uncertainty, and that uncertainty has steadily decreased from 10 to 20 m in 1966, to 5 to 10 m in 1969, to 2 to 8 m in 1973.

E. Formal statistics are generally optimistic, and therefore the uncertainty in coordinates is established by intercomparison, a method that has proved reliable.

F. A comparison between coordinates indicates an accuracy of 2 to 4 m for fundamental stations and 5 to 10 m for most others.

G. The body of laser data available, though small, has made a significant contribution. The laser data dominate the solution through the relatively great weight assigned and thereby essentially establish the reference frame for the station coordinates.

H. The use of a variety of satellite orbits spanning a considerable period of time is very important. Such data average over error sources with a slow variation such as UT1 or epoch timing and eliminate poor orbital geometry. The laser data suffered from both problems.

I. Geometrical data require a minimum of assumptions, and geometrical solutions have relatively straightforward statistics. Geometrical data are more difficult to obtain owing to the necessity of simultaneous observations. Dynamical data are more plentiful, but their processing requires an elaborate orbit-computation program that may introduce model errors. The well-behaved statistical properties of the geometrical data allowed the use of the geometrical networks to establish the uncertainties.

J. Small but significant systematic differences in scale and orientation are found between satellite coordinate systems. These differences may result from variations in data-processing methods or from fundamental differences in the definition of reference systems, e.g., the FK4 system and the JPL planetary ephemeris.

K. Satellite determinations of site location are now sufficiently accurate to verify terrestrial survey data. The most troublesome part of the analysis was finding the erroneous survey coordinates. Considerable effort remains in providing global geodetic coordinates with sufficient reliability.

L. Scale obtained for the four major datums is systematically smaller than the satellite results by 1.6 ± 1 ppm. Since survey scales are not expected to be established to better than a few ppm, this result is not considered to be significantly different from zero.

M. Satellite-tracking data from 25 satellites have been combined with terrestrial gravity data to determine the spherical-harmonic representation of the geopotential complete through degree and order 18, plus several higher harmonics to which satellite orbits are sensitive.

N. The zonal harmonics are successfully determined from analysis of long-period and secular perturbations, while the tesseral and sectorial harmonics are obtained from short-periodic satellite perturbations and terrestrial gravimetry. Low-degree and low-order $\ell, m \leq 8$ are primarily determined from satellite perturbations, and the short-wavelength $\ell, m \geq 8$, primarily from terrestrial gravity data.

O. The principal improvements over Gaposchkin and Lambeck (1970) are due to 1) the addition of two low-inclination satellites for the determination of the zonal harmonics, 2) the use of a sizable number of precise laser observations, and 3) the use of an improved set of terrestrial gravity anomalies.

P. In the combination of satellite and surface-gravity measurements, some attention must be given to the unobserved areas.

Q. The unobserved areas are treated by using anomalies computed from a satellite-determined reference field and by taking the expected value of this residual field as zero, with a large variance.

R. The accuracy of the solution is established by comparison with satellite orbits and with terrestrial gravity data not used in the solution.

S. The lower harmonics have been improved such that the total orbit-computing system has an rms error of between 5 and 10 m for 4-day arcs.

T. The accuracy of the generalized geoid is ≈ 64 mgal^2, or 2.5 m.

U. The geoid is very similar to that found by Gaposchkin and Lambeck (1970); no new features have been found, and none has disappeared. Therefore, geophysical analyses from these results remain valid (see, e.g., Kaula, 1970, 1972; Gaposchkin, Kaula, and Lambeck, 1970).

REFERENCES

Aardoom, L., A. Girnius, and G. Veis, Geometric methods, in Geodetic Parameters for a 1966 Smithsonian Institution Standard Earth, edited by C. A. Lundquist and G. Veis, vol. 1, pp. 63-75, Smithsonian Astrophys. Obs. Spec. Rep. No. 200, 1966.

Aeronautical Chart and Information Center, 1° X 1° Mean Free-Air Gravity Anomalies, ACIC Reference Publ. No. 29, August, 324 pp., 1971.

Gaposchkin, E. M., A dynamical solution for the tesseral harmonics of the geopotential and station coordinates using Baker-Nunn data, in Space Research VII, edited by R. L. Smith-Rose, S. A. Bowhill, and J. W. King, pp. 683-693, North-Holland Publ. Co., Amsterdam, 1967.

Gaposchkin, E. M., Improved values for the tesseral harmonics of the geopotential and station coordinates, in Dynamics of Satellites 1969, edited by B. Morando, pp. 109-118, Springer-Verlag, Berlin, 1970.

Gaposchkin, E. M., Empirical data and the variance-covariance matrix for the 1969 Smithsonian Standard Earth (II), Smithsonian Astrophys. Obs. Spec. Rep. No. 342, 60 pp., 1972.

Gaposchkin, E. M., editor, 1973 Smithsonian Standard Earth (III), Smithsonian Astrophys. Obs. Spec. Rep. No. 353, 388 pp., 1973.

Gaposchkin, E. M., W. M. Kaula, and K. Lambeck, 1969 Smithsonian Standard Earth and global tectonics, in Gravimetric and Geometric Investigations with Geos 1 and Geos 2, vol. I of Proc. Geos Program Review Meeting, edited by Computer Sciences Corp., pp. 7-59, NASA, Washington, D.C., 1970.

Gaposchkin, E. M., and K. Lambeck, 1969 Smithsonian Standard Earth (II), Smithsonian Astrophys. Obs. Spec. Rep. No. 315, 93 pp., 1970.

Gaposchkin, E. M., J. Latimer, and G. Veis, Smithsonian Institution Standard Earth III. Coordinates, presented at the First International Symposium on the Use of Artificial Satellites for Geodesy and Geodynamics, Athens, May, 1973.

Gaposchkin, E. M., M. R. Williamson, Y. Kozai, and G. Mendes, Determination of the geopotential, in 1973 Smithsonian Standard Earth (III), edited by E. M. Gaposchkin, pp. 229-308, Smithsonian Astrophys. Obs. Spec. Rep. No. 353, 1973.

Heiskanen, W. A., and H. Moritz, Physical Geodesy, W. H. Freeman and Co., San
    Francisco, 364 pp., 1967.

Kahle, H. G., and M. Talwani, Gravimetric Indian Ocean geoid, Zs. f. Geophys.,
    39, 167-187, 1973.

Kaula, W. M., Tests and combinations of satellite determinations of the gravity fields
    with gravimetry, J. Geophys. Res., 71, 5303-5314, 1966.

Kaula, W. M., Theory of statistical analysis of data distributed over a sphere, Rev.
    Geophys., 5, 38-107, 1967.

Kaula, W. M., Earth's gravity field: Relation to global tectonics, Science, 169,
    982-985, 1970.

Kaula, W. M., Global gravity and tectonics, in The Nature of the Solid Earth, edited
    by E. C. Robinson, J. F. Hays, and L. Knopoff, pp. 385-405, McGraw-Hill,
    New York, 1972.

Kaula, W. M., and W. Lee, A spherical harmonic analysis of the earth's topography,
    J. Geophys. Res., 72, 753-758, 1967.

Köhnlein, W. J., Corrections to station coordinates and to nonzonal harmonics from
    Baker-Nunn observations, in Space Research VII, edited by R. L. Smith-Rose,
    S. A. Bowhill, and J. W. King, pp. 694-701, North-Holland Publ. Co.,
    Amsterdam, 1967.

Kozai, Y., Effect of precession and nutation on the orbital elements of a close earth
    satellite, Astron. J., 65, 621-623, 1960.

Kozai, Y., New determination of zonal harmonics coefficients of the earth's gravi-
    tational potential, Publ. Astron. Soc. Japan, 16, 263-284, 1964; also in
    Smithsonian Astrophys. Obs. Spec. Rep. No. 165, 38 pp.

Kozai, Y., Revised values for coefficients of zonal spherical harmonics in the
    geopotential, Smithsonian Astrophys. Obs. Spec. Rep. No. 295, 17 pp., 1969.

Lambeck, K., A spatial triangulation solution for a global network and the position
    of the North American Datum within it, presented at the American Geophysical
    Union Meeting, Washington, D.C., April 1969.

Lambeck, K., Comparisons and combinations of geodetic parameters estimated from
    dynamic and geometric satellite solutions and from Mariner flights, in
    Dynamics of Satellites 1969, edited by B. Morando, pp. 170-179, Springer-Verlag,
    Berlin, 1970.

Lehr, C. G., Geodetic and geophysical applications of laser satellite ranging, IEEE Trans. Geos. Elec., GE-7, 261-267, 1969.

Lundquist, C. A., and G. Veis, editors, Geodetic Parameters for a 1966 Smithsonian Institution Standard Earth, Smithsonian Astrophys. Obs. Spec. Rep. No. 200, 3 vols., 686 pp., 1966.

Mather, R., The Australian geodetic datum in earth space, UNISURV Rep. No. 19, p. 80, Univ. New South Wales, 1970.

Mottinger, N., Status of D.S.F. location solution for deep space probe missions, in Space Programs Summary No. 37-60, vol. II, pp. 77-89, Deep Space Network, Jet Propulsion Lab., Pasadena, Calif., 1969.

Mottinger, N., Letter to E. M. Gaposchkin, May 31, 1972.

Mottinger, N., Jet Propulsion Laboratory's contribution to the National Geodetic Satellite Program Document, preprint, Jet Propulsion Lab., Pasadena, Calif., 1973.

Talwani, M., H. R. Poppe, and P. D. Rabinowitz, Gravimetrically determined geoid in the western North Atlantic, in Sea Surface Topography from Space, edited by J. Apel, vol. II, pp. 23-1 to 23-33, NOAA Tech. Rep. ERL 228 - AOML 7-2, 1972.

Trask, D. W., and C. J. Vegos, Intercontinental longitude differences of tracking stations as determined from radio tracking data, in Continental Drift, Secular Motion of the Pole, and Rotation of the Earth, Proc. IAU Symp. No. 32, edited by B. Markowitz and B. Guinot, pp. 91-94, D. Reidel Publ. Co., Dordrecht-Holland, 1968.

Vegos, C. J., and D. W. Trask, Tracking station location as determined by radio tracking data, in Space Programs Summary No. 37-43, vol. III, pp. 11-28, Deep Space Network, Jet Propulsion Lab., Pasadena, Calif., 1967.

Veis, G., Geodetic uses of artificial satellites, Smithsonian Contr. Astrophys., 3, 95-161, 1960.

Veis, G., Relation with DSIF stations, in Geodetic Parameters for a 1966 Smithsonian Institution Standard Earth, edited by C. A. Lundquist and G. Veis, vol. 3, pp. 115-125, Smithsonian Astrophys. Obs. Spec. Rep. No. 200, 1966.

Veis, G., Geodetic interpretation of the results, in Space Research VII, edited by R. L. Smith-Rose, S. A. Bowhill, and J. W. King, pp. 776-777, North-Holland Publ. Co., Amsterdam, 1967a.

Veis, G., Results from geometric methods, in Space Research VII, edited by R. L. Smith-Rose, S. A. Bowhill, and J. W. King, pp. 778-782, North-Holland Publ. Co., Amsterdam, 1967b.

Whipple, F. L., On the satellite geodesy program at the Smithsonian Astrophysical Observatory, in Space Research VII, edited by R. L. Smith-Rose, S. A. Bowhill, and J. W. King, pp. 675-683, North-Holland Publ. Co., Amsterdam, 1967.

Wiener, N., Extrapolation, Interpolation, and Smoothing of Stationary Time Series with Engineering Applications, 160 pp., The MIT Press, Cambridge, Mass., 1966.

Williams, J. G., J. D. Mulholland, and P. L. Bender, Spin-axis distance of the McDonald Observatory, presented at the fall meeting of the American Geophysical Union, San Francisco, December 1972; abstract in Trans. Amer. Geophys. Union, 53, p. 968.

TABLE 1. Dynamical Data Used in SE III

Satellite Number	Name	Inclination	Eccentricity	a (km)	Perigee (km)	Laser observations	Station coordinates	Zonal harmonics	Tesseral harmonics	Number of files
7001701	Dial	5°	0.038	7344	301			x		
7010901	Peole	15	0.017	7070	635	x		x	x	4
6001301	Courier 1B 1960 ν1	28	0.016	7465	965		x	x	x	7
5900101	Vanguard 2 1959 α1	33	0.165	8300	557		x	x	x	7
5900701	1959 η1	33	0.188	8483	515		x			18
6100401	1961 δ1	39	0.119	7960	700				x	4
6701401	D1D	39	0.053	7337	569	x	x		x	10
6701101	D1C	40	0.052	7336	579	x	x		x	9
6503201	Explorer 24 BE-C	41	0.026	7311	941	x	x		x	13
6202901	Telstar 1 1962 αε1	44	0.241	9672	962			x		4
6000902	1960 ι2	47	0.011	7971	1512		x	x	x	10
6206001	Anna 1B 1962 βμ1	50	0.007	7508	1077		x	x	x	12
6302601	Geophysical Research	50	0.062	7237	424			x		6
6508901	Explorer 29 Geos 1	59	0.073	8074	1121	x	x	x	x	56
6101501	Transit 4A 6101	67	0.008	7318	885			x	x	10
6101502	Injun 1 6102	67	0.008	7316	896				x	9
6506301	Secor 5	69	0.079	8159	1137		x		x	2
6400101		70	0.002	7301	921			x	x	4
6406401	Explorer 22 BE-B	80	0.012	7362	912	x	x	x	x	6
6508101	OGO 2	87	0.075	7344	420			x	x	5
6600501	Oscar 07	89	0.023	7417	868		x		x	1
6304902	5BN-2	90	0.005	7473	1070		x		x	5
6102801	Midas 4 1961 αδ1	96	0.013	10005	3503		x	x	x	6
6800201	Explorer 36 Geos 2	106	0.031	7709	1101	x	x		x	13
6507801	OV1-2	144	0.182	8306	416		x		x	4

TABLE 2. DSN Data Used in LS 37

Flight	Tracking time period	δ
Mariner 4 encounter	July 10−21, 1965	−3°
Mariner 5 cruise	July 28−September 16, 1967	−8° to +8°
Mariner 5 encounter	October 14−25, 1967	6°
Mariner 5 post encounter	October 28−November 21, 1967	+2° to −2°
Mariner 6	July 26−31, 1969	−24°

TABLE 3. LS 37 Coordinates, from Mottinger (1973)

Station	r (Mm)	λ	X (Mm)	Y (Mm)
4711	5.2063409	243.°15059	-2.3514288	-4.6450800
4712	5.2120525	243.19452	-2.3504424	-4.6519794
4714	5.2039978	243.11047	-2.3536211	-4.6413425
4741	5.4502019	136.88749	-3.9787186	3.7248488
4742	5.2053494	148.98126	-4.4609782	2.6824124
4751	5.7429399	27.68542	5.0854415	2.6682659
4761	4.8626083	355.75097	4.8492431	-0.3602785
4762	4.8608181	355.63217	4.8467007	-0.3701960

TABLE 4. The Stations Related by Survey

Location	Stations pairs	$1/\sigma^2$ (m^{-2})	Location	Station pairs	$1/\sigma^2$ (m^{-2})
Maryland	7050–6002	1.0	California	4714–4712	5.0
Hawaii	9012–6011	1.0		4714–4711	5.0
Argentina	9011–6019	1.0		9113–4714	0.7
Japan	9005–6013	0.1		9113–6111	2.0
Spain	4761–4762	5.0		6111–6134	5.0
	9004–4761	0.20	Ethiopia	9028–6042	2.0
Central Europe	9066–8015	0.25	Australia	6060–4741	1.0
	9066–6065	0.0025		9003–4741	1.0
	7816–9030	0.01		9003–9023	1.0
Brazil	9029–6067	1.0		4741–4742	0.04
			South Africa	9002–6068	1.0
				9002–4751	0.1

TABLE 5. Distribution of 1° × 1° Mean Gravity Anomalies

Boundary (km)	Ocean		Continent	
	Measured	Total	Measured	Total
0	9213	42918	10115	21882
−1	7015	36199	12313	28601

TABLE 6. The Global Covariance Function, Calculated by Using the
19, 328 1° × 1° Mean Gravity Anomalies

Average angular distance	Covariance function (mgal^2)
0°	1150
0.92	656
1.62	431
2.52	326
3.50	266
4.50	234
5.49	208
6.47	185
7.47	180
8.48	163
9.48	145
10.48	131
11.47	124
12.48	124
13.48	111
14.48	105
15.47	92
16.48	95
17.48	86
18.48	84
19.48	78

TABLE 7. The Block Covariance Function of Unit Gravity Anomalies

Average angular distance	Covariance function (mgal^2)
0°	1078
0.29	604
0.93	662
1.21	505
1.78	420
2.18	329
2.80	278
3.17	251
3.70	246
4.19	211
4.75	179
5.22	168
5.69	200
6.20	− 2
6.69	575

TABLE 8. The Covariance Function of 5° × 5° Mean Block Gravity Anomalies

Average angular distance	Covariance function (mgal^2)
0°	314
4.85	192
7.32	141
12.23	97
17.25	65
22.32	43
27.33	22
32.29	8
37.33	2

TABLE 9. Assumed Accuracy for Data Used in SE III

Data	Weight	Remarks
Baker-Nunn	4"	
Smoothed Baker-Nunn	2"	
SAO laser	5 m	Observed before 1970
Centre National d'Etudes Spatiales laser	10 m	Observed before 1970
GSFC laser	5 m	Observed before 1970
ISAGEX laser	5 m	1971 International Campaign

TABLE 10. Observations Included in the Dynamical Solution

Pre-ISAGEX Data 15 satellites 140 arcs				ISAGEX Data 3 satellites 15 arcs	
Station number	Number of observations	Station number	Number of observations	Station number	Number of observations
7050	274	9011	1637	7050	1425
7818	1223	9012	3088	7060	1514
8015	612	9028	525	7804	625
7815	1970	9029	261	7809	1178
9001	4357	9031	467	7820	296
9002	2120	9021	81	7902	1484
9003	349	9066	809	7907	746
9023	2630	9025	9	7921	225
9004	3343	9080	47	7929	213
9005	945	9091	143	7930	89
9006	3170	7921	9	9030	172
9007	1646	7816	2382	9021	29
9008	2301	7804	200		
9009	1825	7901	761		
9010	2424				

TABLE 11. Adopted Constants

$GM = 3.986013 \times 10^{20}$ cm^3 sec^{-2}

$c = 2.997925 \times 10^{10}$ cm sec^{-1} (velocity of light)

$k_2 = 0.30$ (Love number)

TABLE 12. Additional Parameters Determined

Relation to the dynamical system	Translation parameters (m)	Rotation parameters about the axis (μrad)	Scale parameter
SAO geometrical	$X = -6.66$	$\epsilon_x = 0.70 \pm 1.56$	
	$Y = -14.88$	$\epsilon_y = 0.84 \pm 1.24$	
	$Z = -9.90$	$\epsilon_z = -0.40 \pm 1.43$	
BC-4 geometrical	$X = -11.25 \pm 9.60$	$\epsilon_x = 1.76 \pm 0.96$	
	$Y = -16.63 \pm 9.58$	$\epsilon_y = -0.65 \pm 0.65$	
	$Z = -6.79 \pm 13.74$	$\epsilon_z = -2.20 \pm 0.82$	
JPL		$\epsilon_z = -3.43 \pm 1.02$	$0.18 \times 10^{-6} \pm 0.55 \times 10^{-6}$

TABLE 13. Geocentric Coordinates

Station	X (Mm)	Y (Mm)	Z (Mm)	σ (m)	Location
7050	1.1306739	-4.8313735	3.9941010	1.81	GREENBELT ,USA
1021	1.1180308	-4.8763213	3.9429730	1.81	BLOSSOM POINT,USA
7060	-5.0689641	3.5841051	1.4587443	2.88	GUAM,USA
7816	4.6543369	1.9591790	3.8843585	2.26	STEPHANION,GREECE
7818	-5.4263231	-.2293266	3.3346064	6.07	COLOMB-BECHAR,ALGERIA
8015	4.5783277	.4579748	4.4031797	2.07	HAUTE PROVENCE,FRANCE
7815	4.5783707	.4579591	4.4031355	2.07	HAUTE PROVENCE,FRANCE
7809	4.5783484	.4579659	4.4031579	2.07	HAUTE PROVENCE,FRANCE
9001	-1.5357686	-5.1669390	3.4010425	2.44	ORGAN PASS,USA
7901	-1.5357686	-5.1669890	3.4010425	2.44	ORGAN PASS,USA
9002	5.0561267	2.7165136	-2.7757883	1.79	OLIFANTSFONTEIN,REP.S.AFR.
7902	5.0561265	2.7165135	-2.7757883	1.79	OLIFANTSFONTEIN,REP.S.AFR.
9022	5.0561207	2.7165243	-2.7757870	1.79	OLIFANTSFONTEIN,REP.S.AFR.
9003	-3.9837783	3.7430939	-3.2755610	2.49	WOOMERA,AUSTRALIA
9023	-3.9777568	3.7251061	-3.3030283	2.16	ISLAND LAGOON,AUSTRALIA
9004	5.1055919	-.5552300	3.7696625	3.06	SAN FERNANDO,SPAIN
7804	5.1056120	-.5552523	3.7696312	3.06	SAN FERNANDO,SPAIN
9005	-3.9466906	3.3652957	3.6988334	6.26	TOKYO,JAPAN
9025	-3.9104342	3.3763574	3.7292202	6.26	DODAIRA,JAPAN
9006	1.0182044	5.4711045	3.1096219	2.77	NAINI TAL,INDIA
9007	1.9427769	-5.8040994	-1.7969311	2.11	AREQUIPA,PERU
7907	1.9427770	-5.8040898	-1.7969312	2.11	AREQUIPA,PERU
9027	1.9427718	-5.8040961	-1.7969094	2.11	AREQUIPA,PERU
9008	3.3768929	4.4039823	3.1362578	5.08	SHIRAZ,IRAN
9009	2.2518237	-5.8169157	1.3271635	4.42	CURACAO,ANTILLES
9010	.9762870	-5.6013947	2.8802347	2.86	JUPITER,USA
9011	2.2805913	-4.9145735	-3.3554230	3.19	VILLA DOLORES,ARGENTINA
9012	-5.4660598	-2.4042788	2.2421805	2.72	MAUI,USA
7912	-5.4660630	-2.4042787	2.2421727	2.72	MAUI,USA
9021	-1.9367738	-5.0777083	3.3319024	3.16	MT. HOPKINS,USA
7921	-1.9367727	-5.0777053	3.3319076	3.16	MT. HOPKINS,USA
9023	4.9037652	3.9652160	.9638680	4.85	ADDIS ABABA,ETHIOPIA
9029	5.1864597	-3.6538660	-.6543347	3.86	NATAL,BRAZIL
7929	5.1864599	-3.6538662	-.6543348	3.86	NATAL,BRAZIL
9039	5.1864698	-3.6538452	-.6543344	3.86	NATAL,BRAZIL
9031	1.6938054	-4.1123326	-4.5566531	5.24	COMODORO RIVADAVIA,ARGENTINA
9091	4.5951675	2.0394660	3.9126587	4.11	DIONYSOS,GREECE
7930	4.5952234	2.0394492	3.9126121	4.11	DIONYSOS,GREECE
9030	4.5952145	2.0394480	3.9126220	4.11	DIONYSOS,GREECE
8019	4.5794767	.5866188	4.3864127	10.40	NICE,FRANCE
9066	4.3313047	.5675218	4.6331012	3.67	ZIMMERWALD,SWITZERLAND
9074	3.1838845	1.4214753	5.3228021	20.57	RIGA,LATVIA
9077	3.9074366	1.6024417	4.7638864	83.31	USHGOROD,USSR
9080	3.9201689	-.1347323	5.0127143	13.26	MALVERN,U.K.
9113	-2.4500089	-4.6244149	3.6350288	3.70	ROSAMOND,USA
9114	-1.2648451	-3.4668797	5.1854541	10.87	COLD LAKE,CANADA
9115	3.1212760	.5926423	5.5127109	12.63	HARESTUA,NORWAY
9117	-6.0074079	-1.1118591	1.8257369	7.25	JOHNSTON IS.,USA
4711	-2.3514471	-4.6450706	3.6737600	3.80	CALIFORNIA JPL,USA
4712	-2.3504606	-4.6519699	3.6656247	3.80	CALIFORNIA JPL,USA
4714	-2.3536393	-4.6413332	3.6770483	3.77	CALIFORNIA JPL,USA
4741	-3.9787021	3.7248587	-3.3022081	2.78	AUSTRALIA JPL
4742	-4.4609669	2.6824234	-3.6746138	6.05	AUSTRALIA JPL
4751	5.0854475	2.6682502	-2.7687261	4.73	SO. AFRICA JPL
4761	4.8492411	-.3602972	4.1148673	3.64	SPAIN JPL
4762	4.8466987	-.3702149	4.1168905	3.66	SPAIN JPL
6001	.5465862	-1.3399730	6.1802329	11.15	THULE,GREENLAND
6002	1.1307688	-4.8308360	3.9947002	2.38	BELTSVILLE,USA
6003	-2.1278251	-3.7858474	4.6560279	7.52	MOSES LAKE,USA

TABLE 13. (Cont.)

Station	X (Mm)	Y (Mm)	Z (Mm)	σ (m)	Location
6004	-3.8517699	.3964305	5.0513354	19.38	SHEMYA,USA
6006	2.1029482	.7216791	5.9581765	13.56	TROMSO,NORWAY
6007	4.4336546	-2.2681407	3.9716410	12.86	AZORES,PORTUGAL
6008	3.6232536	-5.2142311	.6015174	12.95	PARAMARIBO,NETHERLAND
6009	1.2808455	-6.2509435	-.0108277	15.17	QUITO,ECUADOR
6011	-5.4660104	-2.4043979	2.2422163	3.12	MAUI,USA
6012	-5.8585251	1.3945295	2.0937902	13.96	WAKE IS.,USA
6013	-3.5658470	4.1207283	3.3034218	7.56	KANOYA,JAPAN
6015	2.6043786	4.4441667	3.7503171	10.37	MASHHAD,IRAN
6016	4.8964136	1.3161788	3.8566662	10.87	CATANIA,ITALY
6019	2.2806429	-4.9145366	-3.3554419	3.54	VILLA DOLORES,ARGENTINA
6020	-1.8886006	-5.3548647	-2.8957716	19.81	EASTER IS.,CHILE
6022	-6.0999436	-.9973208	-1.5685982	12.65	TUTUILA,AM.SAMOA
6023	-4.9553518	3.8422666	-1.1638598	8.96	THURSDAY IS.,AUSTRALIA
6031	-4.3138010	.8913646	-4.5972827	9.29	INVERCARGILL,NEW ZEALAND
6032	-2.3753707	4.8755672	-3.3454056	10.59	CAVERSHAM,AUSTRALIA
6038	-2.1609779	-5.6426947	2.0353523	8.65	REVILLA GIGEDO,MEXICO
6039	-3.7247525	-4.4211985	-2.6861050	22.12	PITCAIRN IS.,U.K.
6040	-.7419364	6.1908105	-1.3385578	13.24	COCOS IS.,AUSTRALIA
6042	4.9007728	3.9682490	.9663303	4.93	ADDIS ABABA,ETHIOPIA
6043	1.3713935	-3.6147358	-5.0559691	12.76	CERRO SOMBRERO,CHILE
6044	1.0989265	3.6846465	-5.0718835	23.43	HEARD IS.,AUSTRALIA
6045	3.2234594	5.0453453	-2.1918119	9.30	MAURITIUS,U.K.
6047	-3.3619221	5.3653261	.7636214	12.76	ZAMBOANGA,PHILIPPINES
6050	1.1926976	-2.4509877	-5.7470744	19.81	PALMER STA.,ANTARCTIC
6051	1.1113619	2.1692821	-5.8743530	13.95	MAWSON STA.,ANTARCTIC
6052	-.9025718	2.4095500	-5.8165695	13.80	WILKES STA.,ANTARCTIC
6053	-1.3108218	.3112360	-6.2132992	13.45	MCMURDO STA.,ANTARCTIC
6055	6.1183495	-1.5717384	-.8786181	11.14	ASCENSION IS.,U.K.
6059	-5.8853237	-2.4483377	.2216584	10.63	CHRISTMAS IS.,U.K.
6060	-4.7516206	2.7920847	-3.2001812	3.19	CULGOORA,AUSTRALIA
6061	2.9999396	-2.2193526	-5.1552794	15.33	SO. GEORGIA,U.K.
6063	5.8844839	-1.8534891	1.6128432	11.17	DAKAR,SENEGAL
6064	6.0234113	1.6179373	1.3317254	9.89	FORT LAMY,CHAD
6065	4.2135852	.8208359	4.7027662	12.59	HOHENPEISSENBERG,W.GERMANY
6067	5.1864154	-3.6539275	-.6542977	4.13	NATAL,BRAZIL
6068	5.0848489	2.6703463	-2.7681144	2.38	JOHANNESBURG,REP.S.AFR.
6069	4.9784430	-1.0868507	-3.8231816	26.56	TRISTAN DA CUNHA,U.K.
6072	-.9416635	5.9674615	2.0393072	13.65	CHIANG MAI,THAILAND
6073	1.9051653	6.0322878	-.8107365	12.02	CHAGOS,ARCHIPELG
6075	3.6028471	5.2382448	-.5159507	11.39	SEYCHELLES,U.K.
6078	-5.9523041	1.2319412	-1.9259390	22.93	NEW HEBRIDES,U.K.
6111	-2.4488492	-4.6679685	3.5827461	3.83	WRIGHTWOOD,USA
6123	-1.8817815	-.8124227	6.0195886	17.73	POINT BARROW,USA
6134	-2.4489029	-4.6680586	3.5824408	3.89	WRIGHTWOOD,USA

TABLE 14. Comparison of BC-4 Geometrical Solution with the Combination Solution (in units of meters). The Standard Error of Unit Weight, σ_0, is 0.823.

Station	Weight	Residual					
		ΔX	ΔY	ΔZ	North	East	Height
6001	12.22	0	0	4	0	0	4
6002	5.54	12	-13	9	1	-15	13
6003	9.03	0	- 4	0	- 2	2	2
6004	20.01	2	- 9	1	3	9	0
6006	14.45	- 6	-12	4	11	-10	0
6007	13.80	- 6	- 5	- 1	1	- 7	- 3
6008	13.88	2	- 4	- 4	- 5	0	4
6009	15.97	5	- 5	- 1	- 1	4	6
6011	5.89	15	4	4	9	2	-13
6012	14.83	7	- 2	1	4	0	- 6
6013	9.06	- 1	- 8	12	13	6	1
6015	11.51	- 5	- 9	7	12	0	- 4
6016	11.96	- 5	-11	3	8	-10	- 4
6019	6.13	13	3	- 5	- 3	13	5
6020	20.43	3	5	- 6	- 8	1	- 2
6022	13.60	7	6	- 1	- 3	- 4	- 8
6023	10.26	- 2	3	0	1	- 1	4
6031	10.55	- 2	4	- 9	- 4	- 4	9
6032	11.71	1	7	- 4	0	- 4	6
6038	9.99	4	5	- 1	0	2	- 6
6039	22.68	4	7	- 4	- 7	- 2	- 5
6040	14.15	- 1	0	0	0	1	0
6042	7.02	- 3	- 7	5	6	- 3	- 6
6043	13.70	11	8	- 8	- 8	13	4
6044	23.96	4	7	- 5	3	- 2	10
6045	10.56	- 5	- 1	- 7	- 8	3	- 1
6047	13.70	0	0	5	5	0	1
6050	20.43	10	2	- 6	0	10	6
6051	14.82	5	4	-10	1	- 2	12
6052	14.68	4	5	- 9	0	- 5	10
6053	14.35	3	5	-12	- 5	- 5	11
6055	12.21	- 9	0	11	10	- 1	-11
6059	11.75	9	5	- 2	- 2	- 1	-11
6060	5.93	- 3	3	- 8	- 5	- 1	8
6061	16.12	8	3	- 4	1	8	6
6063	12.24	- 8	- 2	0	2	- 4	- 7
6064	11.08	- 6	-12	5	7	-10	- 7
6065	13.55	- 6	-12	4	9	-11	- 2
6067	6.49	- 5	13	10	9	7	-13
6068	5.54	- 4	- 3	-24	-24	0	5
6069	27.03	- 8	2	5	0	0	-10
6072	14.54	- 3	- 1	9	9	4	1
6073	13.02	- 7	- 2	0	0	6	- 4
6075	12.44	- 4	- 2	1	1	1	- 4
6078	23.47	- 8	3	9	12	- 1	5
6111	6.30	3	2	7	8	2	1
6123	18.42	1	-13	2	- 3	12	3
6134	6.33	4	12	6	12	- 1	- 7
				rms:	7.35	6.33	7.10
				Total rms:	12.02		

Parameters Determined

	X	Y	Z
Translation (m)	16.32 $\pm$ 1.22	23.21 $\pm$ 1.22	-4.68 $\pm$ 1.22
Rotation	- 0.''101 $\pm$ 0.''050	0.''036 $\pm$ 0.''050	0.''338 $\pm$ 0.''046

Scale (ppm) = 1.17 $\pm$ 0.19

TABLE 15. JPL–SAO Residuals

Rotation: -3.43 ± 1.02 µrad
Scale: $1.8 \times 10^{-7} \pm 5.5 \times 10^{-7}$

Station	R (m)	λ (m)
4711	-0.81	2.69
4712	-0.66	2.63
4714	-0.86	2.57
4741	4.31	-0.21
4742	0.51	1.66
4751	0.96	-3.03
4761	-0.26	2.10
4762	-0.31	2.31

TABLE 16. Translation, Rotation, and Scale Parameters for the Four Major Datums.

Datum	Number of stations	Translation (m)			Rotation			Scale correction (ppm)	σ_0	σ (m)
		X	Y	Z	Azimuth	E–W	N–S			
NA27	10	− 31.4	154.0	176.3	0.″09	−0.″62	−0.″23	1.78	0.67	8
		± 1.9	± 2.2	± 1.9	±0.24	±0.69	±0.24	±1.13		
EU50	17	− 85.4	−111.1	−131.9	0.56	−0.51	−0.22	2.60	0.59	16
		± 2.0	± 1.9	± 2.0	±0.21	±0.35	±0.22	±0.92		
SA69	8	− 75.3	− 3.3	− 52.2	−0.33	−0.13	−0.33	−1.39	0.61	14
		± 2.5	± 2.6	± 2.5	±0.21	±0.27	±0.33	±0.99		
AUGD	7	−118.2	− 38.6	+119.6	0.23	0.82	−0.22	2.33	0.35	5
		± 1.5	± 1.4	± 1.4	±0.26	±0.41	±0.31	±1.22		

TABLE 17. Standard Deviations of Datum-Height Comparisons

Datum	σ (m)
NA27	3.07
SA69	2.69
AUGD	1.25
EU50	8.90
Average:	3.98

TABLE 18. Comparison of Coordinates Determined in Both SE II and SE III. The
Systematic Translation, Rotation, and Scale Differences Were Removed
Before the Residuals Were Computed (in units of meters). The Standard
Error of Unit Weight, σ_0, is 0.662.

Station	Weight	Residual					
		ΔX	ΔY	ΔZ	North	East	Height
7050	7.23	1	− 6	− 9	−12	0	0
8015	5.41	0	7	0	0	7	0
9001	5.58	− 8	4	0	1	− 9	− 1
9002	7.23	1	0	− 3	− 2	− 1	2
9003	6.50	0	0	4	3	0	− 1
9004	5.86	3	− 3	− 4	− 5	− 3	0
9005	11.80	3	− 8	− 1	3	4	− 7
9006	9.42	0	− 2	− 2	− 1	− 1	− 3
9007	7.31	5	−10	3	6	1	10
9008	10.33	− 1	2	6	5	2	4
9009	8.28	− 2	1	4	5	− 1	− 1
9010	5.76	− 1	1	− 4	− 3	− 1	− 3
9011	9.55	5	− 2	5	7	3	1
9012	7.51	− 3	− 1	8	6	0	6
9021	15.33	11	− 6	−13	−13	12	− 5
9023	6.38	1	− 2	5	3	0	− 5
9028	12.94	14	11	− 4	− 6	0	17
9029	12.61	0	−11	− 7	− 7	− 9	7
9031	15.89	5	− 7	− 1	5	2	7
9066	7.90	− 5	8	7	8	9	2
9080	16.03	− 9	4	5	11	3	− 1
9113	7.92	4	3	− 6	− 2	2	− 8
9114	16.19	− 5	2	−13	− 7	− 5	−11
9115	21.18	− 4	− 2	8	8	− 1	5
9117	16.66	− 2	− 4	5	4	4	4

rms: 6.62   5.02   6.37

Total rms: 10.47

Parameters Determined

	X	Y	Z
Translation (m)	−1.69 ± 1.19	3.76 ± 1.18	0.04 ± 1.18
Rotation	−0″039 ± 0″047	−0″043 ± 0″049	−0″059 ± 0″044

Scale (ppm) = −0.26 ± 0.18

TABLE 19. Zonal Harmonics in Fully Normalized Form. $\overline{C}_{\ell,0} = -J_{\ell}/\sqrt{2\ell + 1}.$

Harmonic	Value	Harmonic	Value
$\overline{C}_{2,0}$	-4.84170E-04	$\overline{C}_{14,0}$	-1.94980E-08
$\overline{C}_{3,0}$	9.60408E-07	$\overline{C}_{15,0}$	-1.88586E-08
$\overline{C}_{4,0}$	5.39333E-07	$\overline{C}_{16,0}$	-5.91864E-09
$\overline{C}_{5,0}$	6.87446E-08	$\overline{C}_{17,0}$	3.71868E-08
$\overline{C}_{6,0}$	-1.53097E-07	$\overline{C}_{18,0}$	1.67687E-08
$\overline{C}_{7,0}$	9.08860E-08	$\overline{C}_{19,0}$	-1.58527E-08
$\overline{C}_{8,0}$	4.97198E-08	$\overline{C}_{20,0}$	1.85847E-08
$\overline{C}_{9,0}$	3.53300E-08	$\overline{C}_{21,0}$	1.26574E-08
$\overline{C}_{10,0}$	5.17176E-08	$\overline{C}_{22,0}$	-1.37146E-08
$\overline{C}_{11,0}$	-6.50565E-08	$\overline{C}_{23,0}$	-2.11504E-08
$\overline{C}_{12,0}$	3.84000E-08	$\overline{C}_{35,0}$	1.59029E-08
$\overline{C}_{13,0}$	6.52406E-08	$\overline{C}_{36,0}$	-2.32912E-08

TABLE 20. Resonant Periods

Resonant with order (m)	Satellite	Inclination	Period (days)
9	6102801	95°	2.90
12	6100401	39	15.0
12	6000902	47	15.5
12	6508901	59	7.2
12	6506301	69	3.3
12	6507801	144	2.3
13	6701401	39	9.4, 10.9, 13.1, ...
13	6503201	41	5.6
13	6701101	40	1.6
13	6206001	50	5.3
13	6800201	105	6.3
13	6600501	89	1.8
13	6304901	90	2.5
14	6701101	40	2.6
14	6302601	50	12.2
14	6101501	67	3.84
14	6101502	67	3.76
14	6400101	70	4.9
14	6406401	80	2.9
14	6408101	87	3.8
14	6600501	89	2.2

TABLE 21. Assumed Accuracy for Determination of the Geopotential.

Data	Weight	Remarks
Baker–Nunn	4"	
Smoothed Baker–Nunn	2"	
SAO laser	5 m	Taken before 1970, observed before 1970
CNES laser	10 m	Taken before 1970, observed before 1970
GSFC laser	5 m	Taken before 1970, observed before 1970
ISAGEX laser	2 m	1971 International Campaign
Gravity anomalies	$\langle A \rangle \dfrac{13.5}{nA}$ mgal	n is the number of 1° × 1° squares in each 5° × 5° mean
Model (zero) anomalies	$\langle A \rangle \dfrac{27}{A}$ mgal	A is the area

TABLE 22. Fully Normalized Tesseral-Harmonic Coefficients for the Geopotential

Harmonic	Value	Harmonic	Value	Harmonic	Value	Harmonic	Value
$\overline{C}_{2,2}$	2.3799E-06	$\overline{S}_{2,2}$	-1.3656E-06	$\overline{C}_{3,1}$	1.9977E-06	$\overline{S}_{3,1}$	2.2337E-07
$\overline{C}_{3,2}$	7.7830E-07	$\overline{S}_{3,2}$	-7.5519E-07	$\overline{C}_{3,3}$	4.9011E-07	$\overline{S}_{3,3}$	1.5283E-06
$\overline{C}_{4,1}$	-5.1748E-07	$\overline{S}_{4,1}$	-4.8140E-07	$\overline{C}_{4,2}$	3.4296E-07	$\overline{S}_{4,2}$	6.7174E-07
$\overline{C}_{4,3}$	1.0390E-06	$\overline{S}_{4,3}$	-1.1923E-07	$\overline{C}_{4,4}$	-1.0512E-07	$\overline{S}_{4,4}$	3.5661E-07
$\overline{C}_{5,1}$	-5.3667E-08	$\overline{S}_{5,1}$	-7.9973E-08	$\overline{C}_{5,2}$	5.9869E-07	$\overline{S}_{5,2}$	-3.9910E-07
$\overline{C}_{5,3}$	-5.8429E-07	$\overline{S}_{5,3}$	-1.6338E-07	$\overline{C}_{5,4}$	-1.1583E-07	$\overline{S}_{5,4}$	-4.5393E-08
$\overline{C}_{5,5}$	1.3956E-07	$\overline{S}_{5,5}$	-8.6841E-07	$\overline{C}_{6,1}$	-7.2166E-08	$\overline{S}_{6,1}$	1.7756E-08
$\overline{C}_{6,2}$	2.4670E-08	$\overline{S}_{6,2}$	-4.0654E-07	$\overline{C}_{6,3}$	4.4139E-09	$\overline{S}_{6,3}$	2.9055E-08
$\overline{C}_{6,4}$	-1.0003E-07	$\overline{S}_{6,4}$	-3.0297E-07	$\overline{C}_{6,5}$	-1.3504E-07	$\overline{S}_{6,5}$	-6.0964E-07
$\overline{C}_{6,6}$	-2.9136E-08	$\overline{S}_{6,6}$	-2.6327E-07	$\overline{C}_{7,1}$	2.3532E-07	$\overline{S}_{7,1}$	5.5634E-08
$\overline{C}_{7,2}$	2.0425E-07	$\overline{S}_{7,2}$	1.7321E-07	$\overline{C}_{7,3}$	2.1994E-07	$\overline{S}_{7,3}$	-3.4644E-07
$\overline{C}_{7,4}$	-2.8617E-07	$\overline{S}_{7,4}$	-2.7738E-07	$\overline{C}_{7,5}$	3.4727E-08	$\overline{S}_{7,5}$	8.7014E-08
$\overline{C}_{7,6}$	-2.7496E-07	$\overline{S}_{7,6}$	8.5865E-08	$\overline{C}_{7,7}$	-2.4856E-08	$\overline{S}_{7,7}$	-8.8968E-09
$\overline{C}_{8,1}$	1.0946E-08	$\overline{S}_{8,1}$	4.8429E-08	$\overline{C}_{8,2}$	1.1084E-07	$\overline{S}_{8,2}$	1.0359E-07
$\overline{C}_{8,3}$	-8.8578E-08	$\overline{S}_{8,3}$	-5.0715E-08	$\overline{C}_{8,4}$	-2.2315E-07	$\overline{S}_{8,4}$	2.6511E-07
$\overline{C}_{8,5}$	1.5318E-07	$\overline{S}_{8,5}$	8.1158E-08	$\overline{C}_{8,6}$	-9.7542E-08	$\overline{S}_{8,6}$	2.8082E-07
$\overline{C}_{8,7}$	2.0498E-07	$\overline{S}_{8,7}$	2.4592E-07	$\overline{C}_{8,8}$	1.6967E-07	$\overline{S}_{8,8}$	9.3261E-08
$\overline{C}_{9,1}$	1.8099E-07	$\overline{S}_{9,1}$	4.1091E-08	$\overline{C}_{9,2}$	-2.2013E-08	$\overline{S}_{9,2}$	2.4215E-08
$\overline{C}_{9,3}$	-9.9252E-08	$\overline{S}_{9,3}$	-2.3085E-08	$\overline{C}_{9,4}$	-4.0867E-08	$\overline{S}_{9,4}$	-3.8525E-08
$\overline{C}_{9,5}$	-5.8957E-08	$\overline{S}_{9,5}$	3.6834E-09	$\overline{C}_{9,6}$	4.8812E-08	$\overline{S}_{9,6}$	1.1115E-07
$\overline{C}_{9,7}$	-1.9880E-07	$\overline{S}_{9,7}$	-1.4978E-07	$\overline{C}_{9,8}$	2.3523E-07	$\overline{S}_{9,8}$	9.6355E-09
$\overline{C}_{9,9}$	-3.4533E-08	$\overline{S}_{9,9}$	5.9502E-08	$\overline{C}_{10,1}$	8.9008E-08	$\overline{S}_{10,1}$	-6.0157E-08
$\overline{C}_{10,2}$	-3.7256E-08	$\overline{S}_{10,2}$	-6.3676E-08	$\overline{C}_{10,3}$	-1.3307E-07	$\overline{S}_{10,3}$	-7.2728E-08

TABLE 22. (Cont.)

Harmonic	Value	Harmonic	Value	Harmonic	Value	Harmonic	Value
$\overline{C}_{10,4}$	-2.1887E-08	$\overline{S}_{10,4}$	-7.8408E-08	$\overline{C}_{10,5}$	-6.1509E-09	$\overline{S}_{10,5}$	-1.1904E-07
$\overline{C}_{10,6}$	-9.4142E-08	$\overline{S}_{10,6}$	-1.1728E-08	$\overline{C}_{10,7}$	1.8525E-07	$\overline{S}_{10,7}$	2.1656E-08
$\overline{C}_{10,8}$	1.0887E-09	$\overline{S}_{10,8}$	7.0781E-09	$\overline{C}_{10,9}$	7.8473E-08	$\overline{S}_{10,9}$	5.6381E-09
$\overline{C}_{10,10}$	1.3321E-07	$\overline{S}_{10,10}$	9.8839E-08	$\overline{C}_{11,1}$	-1.2194E-08	$\overline{S}_{11,1}$	7.5463E-08
$\overline{C}_{11,2}$	-2.0255E-08	$\overline{S}_{11,2}$	-6.2998E-08	$\overline{C}_{11,3}$	-1.0988E-09	$\overline{S}_{11,3}$	-3.8098E-08
$\overline{C}_{11,4}$	1.5676E-08	$\overline{S}_{11,4}$	-1.9551E-07	$\overline{C}_{11,5}$	-1.8591E-09	$\overline{S}_{11,5}$	6.1113E-08
$\overline{C}_{11,6}$	6.3601E-08	$\overline{S}_{11,6}$	-2.6457E-08	$\overline{C}_{11,7}$	-3.3761E-08	$\overline{S}_{11,7}$	-1.2825E-07
$\overline{C}_{11,8}$	-1.3634E-08	$\overline{S}_{11,8}$	4.5229E-08	$\overline{C}_{11,9}$	2.1256E-08	$\overline{S}_{11,9}$	6.6721E-08
$\overline{C}_{11,10}$	5.2555E-08	$\overline{S}_{11,10}$	-7.7401E-08	$\overline{C}_{11,11}$	8.6996E-08	$\overline{S}_{11,11}$	-2.5691E-08
$\overline{C}_{12,1}$	-5.6935E-08	$\overline{S}_{12,1}$	-6.6159E-08	$\overline{C}_{12,2}$	-9.7424E-08	$\overline{S}_{12,2}$	4.6341E-08
$\overline{C}_{12,3}$	1.1555E-07	$\overline{S}_{12,3}$	-4.8666E-08	$\overline{C}_{12,4}$	-5.0379E-08	$\overline{S}_{12,4}$	5.3568E-08
$\overline{C}_{12,5}$	8.1834E-08	$\overline{S}_{12,5}$	2.7932E-08	$\overline{C}_{12,6}$	-2.1177E-08	$\overline{S}_{12,6}$	3.5034E-08
$\overline{C}_{12,7}$	2.9751E-08	$\overline{S}_{12,7}$	3.1783E-08	$\overline{C}_{12,8}$	4.0190E-08	$\overline{S}_{12,8}$	5.6877E-08
$\overline{C}_{12,9}$	-1.1503E-07	$\overline{S}_{12,9}$	1.4508E-08	$\overline{C}_{12,10}$	-4.5921E-08	$\overline{S}_{12,10}$	-4.3264E-08
$\overline{C}_{12,11}$	-7.8443E-09	$\overline{S}_{12,11}$	-4.7858E-08	$\overline{C}_{12,12}$	-2.7617E-08	$\overline{S}_{12,12}$	-1.6808E-08
$\overline{C}_{13,1}$	8.6136E-09	$\overline{S}_{13,1}$	-3.2401E-08	$\overline{C}_{13,2}$	-1.0679E-08	$\overline{S}_{13,2}$	-9.0670E-08
$\overline{C}_{13,3}$	-3.2361E-08	$\overline{S}_{13,3}$	4.9286E-08	$\overline{C}_{13,4}$	3.9852E-08	$\overline{S}_{13,4}$	-1.0608E-07
$\overline{C}_{13,5}$	4.0047E-08	$\overline{S}_{13,5}$	3.8114E-08	$\overline{C}_{13,6}$	-2.1906E-08	$\overline{S}_{13,6}$	-1.1321E-08
$\overline{C}_{13,7}$	-7.6933E-08	$\overline{S}_{13,7}$	1.1140E-08	$\overline{C}_{13,8}$	-2.7448E-09	$\overline{S}_{13,8}$	1.4309E-08
$\overline{C}_{13,9}$	-1.1588E-08	$\overline{S}_{13,9}$	7.2989E-08	$\overline{C}_{13,10}$	4.1979E-09	$\overline{S}_{13,10}$	7.6769E-09
$\overline{C}_{13,11}$	-5.4381E-08	$\overline{S}_{13,11}$	1.3450E-08	$\overline{C}_{13,12}$	-4.6633E-08	$\overline{S}_{13,12}$	7.9963E-08
$\overline{C}_{13,13}$	-6.8944E-08	$\overline{S}_{13,13}$	7.1891E-08	$\overline{C}_{14,1}$	-1.4359E-08	$\overline{S}_{14,1}$	5.2390E-08

TABLE 22. (Cont.)

Harmonic	Value	Harmonic	Value	Harmonic	Value	Harmonic	Value
$\overline{C}_{14,2}$	-1.5908E-08	$\overline{S}_{14,2}$	2.7374E-08	$\overline{C}_{14,3}$	9.6915E-08	$\overline{S}_{14,3}$	-2.5631E-08
$\overline{C}_{14,4}$	-2.9864E-08	$\overline{S}_{14,4}$	-3.8189E-09	$\overline{C}_{14,5}$	-1.3828E-09	$\overline{S}_{14,5}$	-5.8680E-08
$\overline{C}_{14,6}$	-1.3872E-08	$\overline{S}_{14,6}$	-2.7976E-08	$\overline{C}_{14,7}$	7.1056E-08	$\overline{S}_{14,7}$	2.4043E-09
$\overline{C}_{14,8}$	-1.8779E-08	$\overline{S}_{14,8}$	-5.8750E-08	$\overline{C}_{14,9}$	-2.4322E-08	$\overline{S}_{14,9}$	6.0461E-08
$\overline{C}_{14,10}$	2.8985E-08	$\overline{S}_{14,10}$	-3.4224E-08	$\overline{C}_{14,11}$	8.2611E-08	$\overline{S}_{14,11}$	-1.9627E-09
$\overline{C}_{14,12}$	1.1751E-09	$\overline{S}_{14,12}$	-3.0967E-08	$\overline{C}_{14,13}$	3.0793E-08	$\overline{S}_{14,13}$	4.7620E-08
$\overline{C}_{14,14}$	-6.5969E-08	$\overline{S}_{14,14}$	3.3030E-09	$\overline{C}_{15,1}$	2.9358E-08	$\overline{S}_{15,1}$	-1.6691E-08
$\overline{C}_{15,2}$	-1.2291E-08	$\overline{S}_{15,2}$	-6.8963E-08	$\overline{C}_{15,3}$	-5.8921E-08	$\overline{S}_{15,3}$	4.4772E-08
$\overline{C}_{15,4}$	1.4876E-08	$\overline{S}_{15,4}$	7.0359E-09	$\overline{C}_{15,5}$	3.6806E-08	$\overline{S}_{15,5}$	-8.4051E-09
$\overline{C}_{15,6}$	1.0081E-08	$\overline{S}_{15,6}$	-3.0473E-08	$\overline{C}_{15,7}$	3.0439E-08	$\overline{S}_{15,7}$	1.5775E-08
$\overline{C}_{15,8}$	-6.8884E-08	$\overline{S}_{15,8}$	6.0808E-08	$\overline{C}_{15,9}$	-4.5169E-08	$\overline{S}_{15,9}$	5.5556E-08
$\overline{C}_{15,10}$	6.2126E-08	$\overline{S}_{15,10}$	-7.1799E-09	$\overline{C}_{15,11}$	-4.4724E-08	$\overline{S}_{15,11}$	-3.4391E-09
$\overline{C}_{15,12}$	-4.2025E-08	$\overline{S}_{15,12}$	5.9072E-09	$\overline{C}_{15,13}$	-4.1654E-08	$\overline{S}_{15,13}$	-5.5892E-09
$\overline{C}_{15,14}$	9.5654E-09	$\overline{S}_{15,14}$	-2.7145E-08	$\overline{C}_{15,15}$	-5.6358E-08	$\overline{S}_{15,15}$	3.4895E-08
$\overline{C}_{16,1}$	-9.9588E-09	$\overline{S}_{16,1}$	5.4160E-08	$\overline{C}_{16,2}$	5.5086E-09	$\overline{S}_{16,2}$	4.9455E-08
$\overline{C}_{16,3}$	5.4189E-08	$\overline{S}_{16,3}$	5.4887E-09	$\overline{C}_{16,4}$	4.6176E-08	$\overline{S}_{16,4}$	3.6270E-08
$\overline{C}_{16,5}$	-2.4432E-08	$\overline{S}_{16,5}$	2.9671E-08	$\overline{C}_{16,6}$	-3.7203E-09	$\overline{S}_{16,6}$	-2.0786E-08
$\overline{C}_{16,7}$	-2.2794E-09	$\overline{S}_{16,7}$	3.0609E-09	$\overline{C}_{16,8}$	-1.0459E-07	$\overline{S}_{16,8}$	-4.4731E-08
$\overline{C}_{16,9}$	2.4845E-08	$\overline{S}_{16,9}$	-8.6262E-08	$\overline{C}_{16,10}$	-3.9928E-08	$\overline{S}_{16,10}$	-4.5058E-09
$\overline{C}_{16,11}$	-2.0848E-08	$\overline{S}_{16,11}$	2.9738E-08	$\overline{C}_{16,12}$	1.5930E-08	$\overline{S}_{16,12}$	-1.2703E-08
$\overline{C}_{16,13}$	2.5280E-08	$\overline{S}_{16,13}$	6.6240E-09	$\overline{C}_{16,14}$	-1.4852E-08	$\overline{S}_{16,14}$	-8.1713E-09
$\overline{C}_{16,15}$	-7.7425E-08	$\overline{S}_{16,15}$	-2.6491E-08	$\overline{C}_{16,16}$	-1.8538E-08	$\overline{S}_{16,16}$	-2.2310E-08

TABLE 22 (Cont.)

Harmonic	Value	Harmonic	Value	Harmonic	Value	Harmonic	Value
$\overline{C}_{17,1}$	8.6593E-09	$\overline{S}_{17,1}$	-4.1093E-08	$\overline{C}_{17,2}$	-9.0769E-09	$\overline{S}_{17,2}$	-2.7205E-08
$\overline{C}_{17,3}$	-7.7864E-09	$\overline{S}_{17,3}$	-1.7913E-08	$\overline{C}_{17,4}$	-4.3231E-08	$\overline{S}_{17,4}$	6.8203E-08
$\overline{C}_{17,5}$	4.1513E-08	$\overline{S}_{17,5}$	-2.5453E-08	$\overline{C}_{17,6}$	-4.5453E-08	$\overline{S}_{17,6}$	-1.7273E-08
$\overline{C}_{17,7}$	1.6938E-08	$\overline{S}_{17,7}$	-3.3752E-08	$\overline{C}_{17,8}$	4.1231E-08	$\overline{S}_{17,8}$	5.8792E-09
$\overline{C}_{17,9}$	-4.3119E-08	$\overline{S}_{17,9}$	-1.5974E-08	$\overline{C}_{17,10}$	-1.0844E-08	$\overline{S}_{17,10}$	5.5628E-08
$\overline{C}_{17,11}$	-4.4136E-08	$\overline{S}_{17,11}$	-4.3123E-09	$\overline{C}_{17,12}$	3.1661E-08	$\overline{S}_{17,12}$	6.2982E-09
$\overline{C}_{17,13}$	2.5147E-08	$\overline{S}_{17,13}$	9.7728E-09	$\overline{C}_{17,14}$	-5.5945E-09	$\overline{S}_{17,14}$	7.2604E-09
$\overline{C}_{17,15}$	4.9113E-08	$\overline{S}_{17,15}$	3.1958E-08	$\overline{C}_{17,16}$	-2.3540E-08	$\overline{S}_{17,16}$	-1.5882E-08
$\overline{C}_{17,17}$	-9.0191E-08	$\overline{S}_{17,17}$	-9.4775E-09	$\overline{C}_{18,1}$	-2.3557E-08	$\overline{S}_{18,1}$	-7.4536E-08
$\overline{C}_{18,2}$	-9.4249E-09	$\overline{S}_{18,2}$	3.0353E-08	$\overline{C}_{18,3}$	-3.5003E-08	$\overline{S}_{18,3}$	-2.0464E-08
$\overline{C}_{18,4}$	2.9433E-08	$\overline{S}_{18,4}$	-4.4672E-08	$\overline{C}_{18,5}$	1.7511E-09	$\overline{S}_{18,5}$	-6.0367E-09
$\overline{C}_{18,6}$	2.3931E-08	$\overline{S}_{18,6}$	-4.4966E-09	$\overline{C}_{18,7}$	-7.8040E-10	$\overline{S}_{18,7}$	-8.2010E-09
$\overline{C}_{18,8}$	5.3819E-08	$\overline{S}_{18,8}$	-2.2106E-08	$\overline{C}_{18,9}$	-3.6120E-10	$\overline{S}_{18,9}$	-5.0562E-09
$\overline{C}_{18,10}$	4.2146E-08	$\overline{S}_{18,10}$	7.8924E-09	$\overline{C}_{18,11}$	2.4981E-08	$\overline{S}_{18,11}$	2.3183E-08
$\overline{C}_{18,12}$	-6.2242E-09	$\overline{S}_{18,12}$	6.6025E-09	$\overline{C}_{18,13}$	-2.6685E-08	$\overline{S}_{18,13}$	-4.2500E-08
$\overline{C}_{18,14}$	9.1191E-09	$\overline{S}_{18,14}$	-3.3129E-08	$\overline{C}_{18,15}$	-4.1521E-08	$\overline{S}_{18,15}$	-1.7610E-08
$\overline{C}_{18,16}$	2.4850E-08	$\overline{S}_{18,16}$	-4.8182E-09	$\overline{C}_{18,17}$	3.5357E-08	$\overline{S}_{18,17}$	-4.7166E-08
$\overline{C}_{18,18}$	-3.4701E-10	$\overline{S}_{18,18}$	5.0554E-08	$\overline{C}_{19,12}$	3.6058E-08	$\overline{S}_{19,12}$	-3.4421E-09
$\overline{C}_{19,13}$	9.6876E-09	$\overline{S}_{19,13}$	-6.6095E-08	$\overline{C}_{19,14}$	7.6389E-09	$\overline{S}_{19,14}$	-2.7649E-08
$\overline{C}_{20,13}$	2.7630E-08	$\overline{S}_{20,13}$	3.2389E-08	$\overline{C}_{20,14}$	3.3687E-08	$\overline{S}_{20,14}$	-6.5741E-08
$\overline{C}_{21,13}$	-1.9799E-08	$\overline{S}_{21,13}$	-3.0711E-08	$\overline{C}_{21,14}$	1.6623E-08	$\overline{S}_{21,14}$	8.7215E-09
$\overline{C}_{22,13}$	-7.9435E-09	$\overline{S}_{22,13}$	4.1452E-09	$\overline{C}_{22,14}$	2.8516E-09	$\overline{S}_{22,14}$	-4.2148E-08
$\overline{C}_{23,13}$	-1.3236E-08	$\overline{S}_{23,13}$	-4.8892E-09	$\overline{C}_{23,14}$	-2.1148E-08	$\overline{S}_{23,14}$	2.2010E-08
$\overline{C}_{24,14}$	3.4668E-09	$\overline{S}_{24,14}$	2.2983E-08				

TABLE 23. Comparison of SE III with Satellite Observations

Epoch (MJD)	σ(m)	n	Epoch (MJD)	σ(m)	n
6508901 (Geos A), A/M = 0.05 cgs					
41000	4.1	289	41010	7.7	523
41002	5.5	367	41012	9.8	577
41004	3.2	314	41014	9.2	715
41006	8.9	601	14016	4.1	425
41008	10.6	696	41018	3.6	221
6800201 (Geos B), A/M = 0.05 cgs					
41038	2.4	249	41046	2.7	441
41040	6.5	533	41048	3.8	304
41042	7.8	681	41052	2.8	388
41044	6.3	651	41054	6.6	602
6701401 (D1D), A/M = 0.1 cgs					
41072	10.3	467	41080	7.4	621
41074	9.9	332	41082	6.9	764
41076	16.3	341	41084	4.9	427
41078	17.0	254	41086	3.6	519

TABLE 24. Comparison of SE III Combination Solution with Surface Gravity (in mgal^2)

Solution	ℓ, m	$\langle (g_t - g_s)^2 \rangle$	$\langle g_t g_s \rangle$	$\langle g_s^2 \rangle$	D	$\langle g_t^2 \rangle$	$E(\epsilon_s^2)$	$E(\epsilon_t^2)$	$E(\delta g^2)$	n^*
SE II[†]	16	75	184	186	163	253	2	11	63	≥ 20
SE II	16	187	177	229	203	311	52	13	122	(306 anomalies)
SE III	18	105	221	236	237	311	15	13	77	
SE III	10	195	150	192	163	302	42	24	129	≥ 1
	14	174	174	220	198	302	47	24	103	(1183 anomalies)
	18	156	202	258	237	302	56	24	75	
SE III	10	184	183	205	163	345	22	19	143	≥ 10
	14	151	215	236	198	345	20	19	111	(659 anomalies)
	18	117	255	281	237	345	26	19	63	
SE III	10	186	151	176	163	311	25 (24)	13	148	≥ 20
	14	146	182	200	198	311	17 (21)	13	116	(306 anomalies)
	18	105	221	236	237	311	15 (18)	13	77	

[*]n is the number of $1° \times 1°$ mean gravity anomalies used to obtain the $5° \times 5°$ mean gravity anomalies.

[†]From the available data, there were 935, 369, and 136 gravity anomalies with $n \geq 1$, 10, and 20 $1° \times 1°$ anomalies.

TABLE 25. Surface-Gravity Residuals for an $l = m = 36$ Potential from Numerical Quadrature (in $mgal^2$)

Degree of reference field	$\langle (g_t - g_s)^2 \rangle$		$\langle (g_s - g_{ref})^2 \rangle$	$E(\epsilon_s^2)$
	$n \geq 1$	$n \geq 20$	$n = 0$	
0	28	29	12	
6	38	39	12	10
8	53	54	20	25
10	56	53	21	24
14	61	50	19	21
18	70	48	16	18
Anomalies used:	1183	306	471	

TABLE 26. Comparison with Independent Surface-Gravity Data (in mgal^2)

Comparison field, g_s	Maximum ℓ, m	n	$\langle(g_t - g_s)^2\rangle$	$\langle g_t g_s\rangle$	$\langle g_s^2\rangle$	D	$\langle g_t^2\rangle$	$E(\epsilon_s^2)$	$E(\epsilon_t^2)$	$E(\delta_g^2)$	Region
SE III	18	3726	147	209	284	237	282	75	13	59	North Atlantic
SE III	18	1794	145	188	232	237	290	44	13	88	Indian Ocean
Averages								$64 \approx 2.5$ m		68	
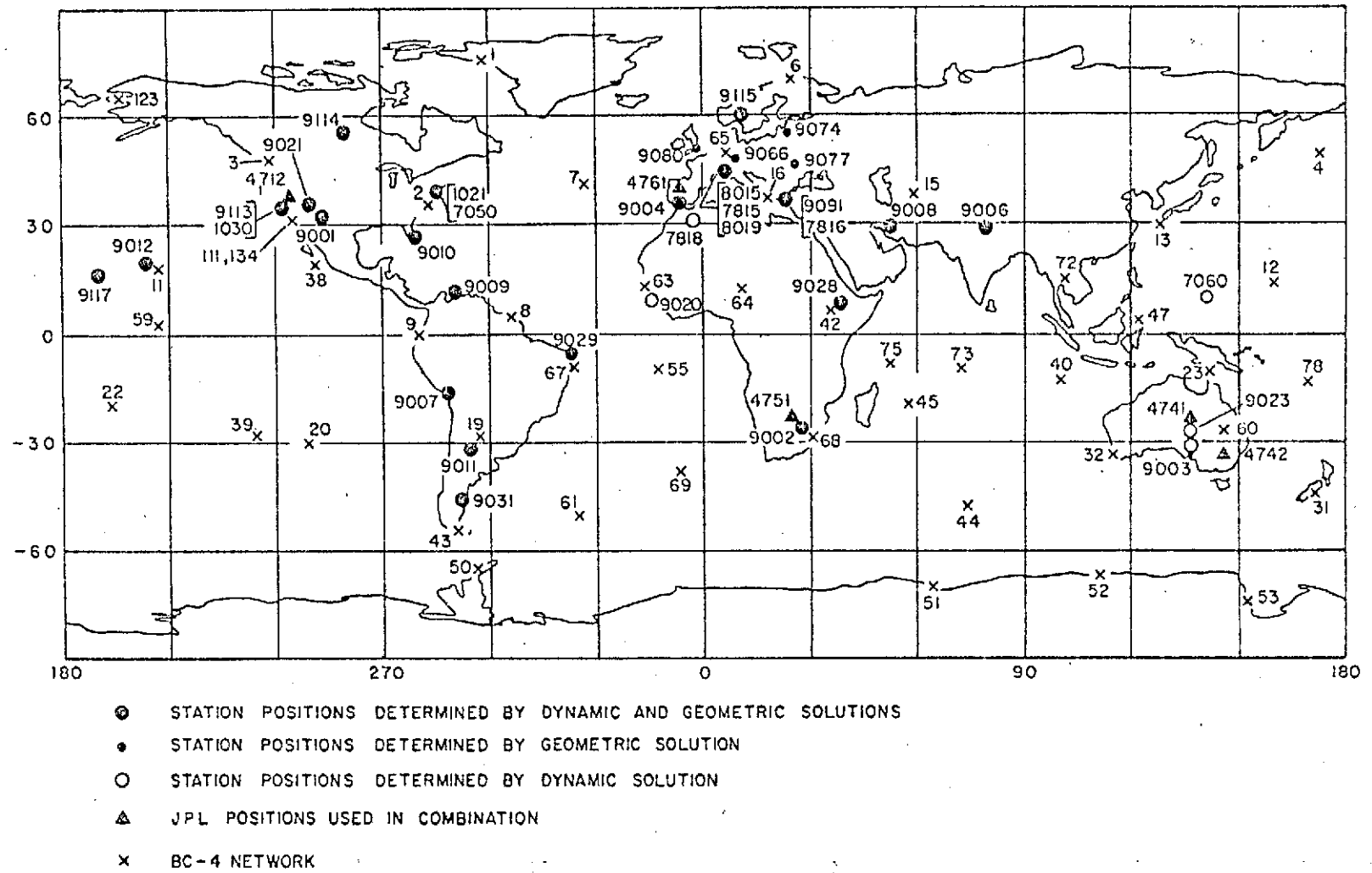
Fig. 1.   Locations of the observing stations included in SE III.
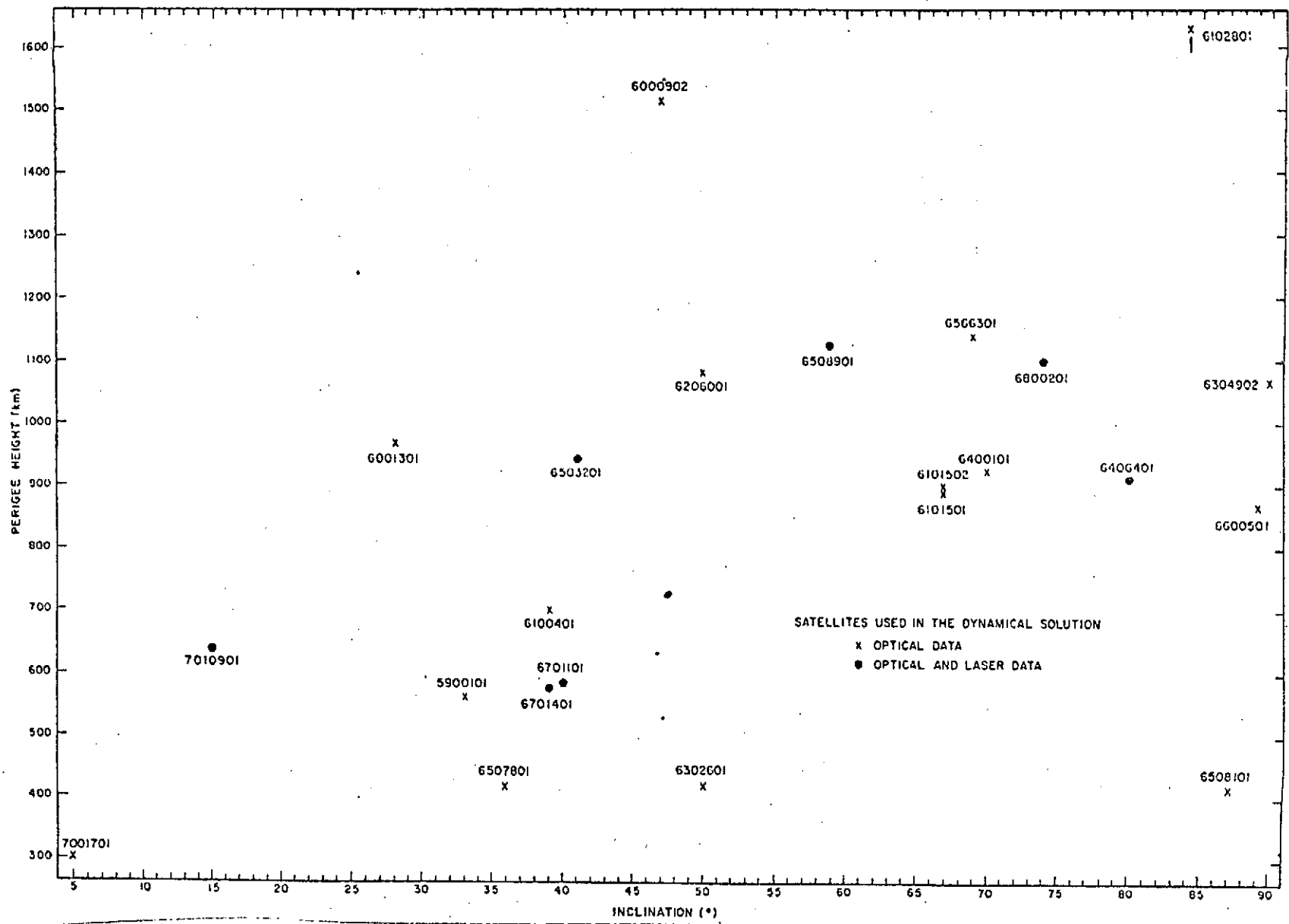
Fig. 2. Distribution of perigee heights and inclinations of the satellites used in SE III.
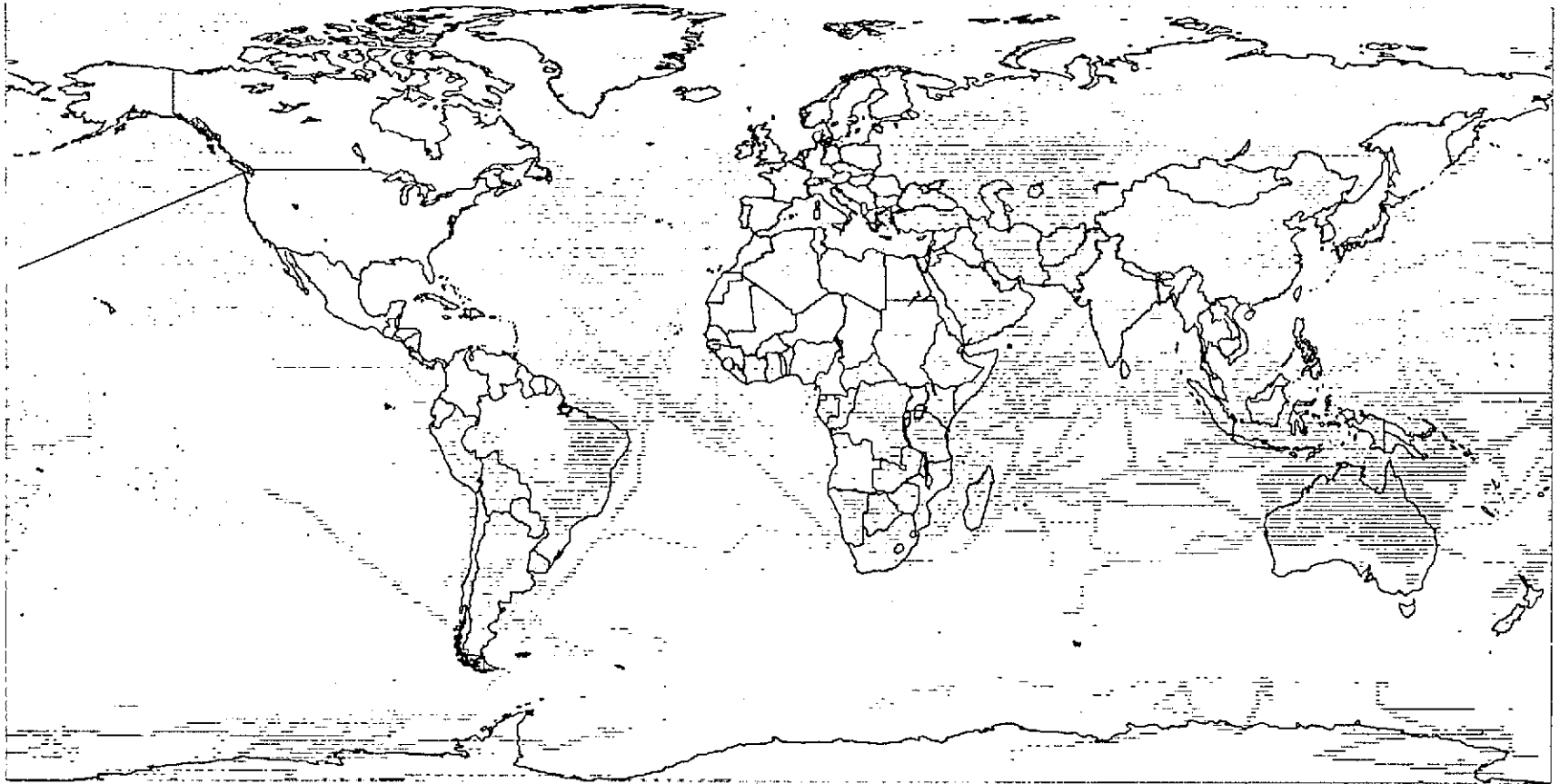
Fig. 3. Distribution of 1°. X 1° mean surface-gravity data.
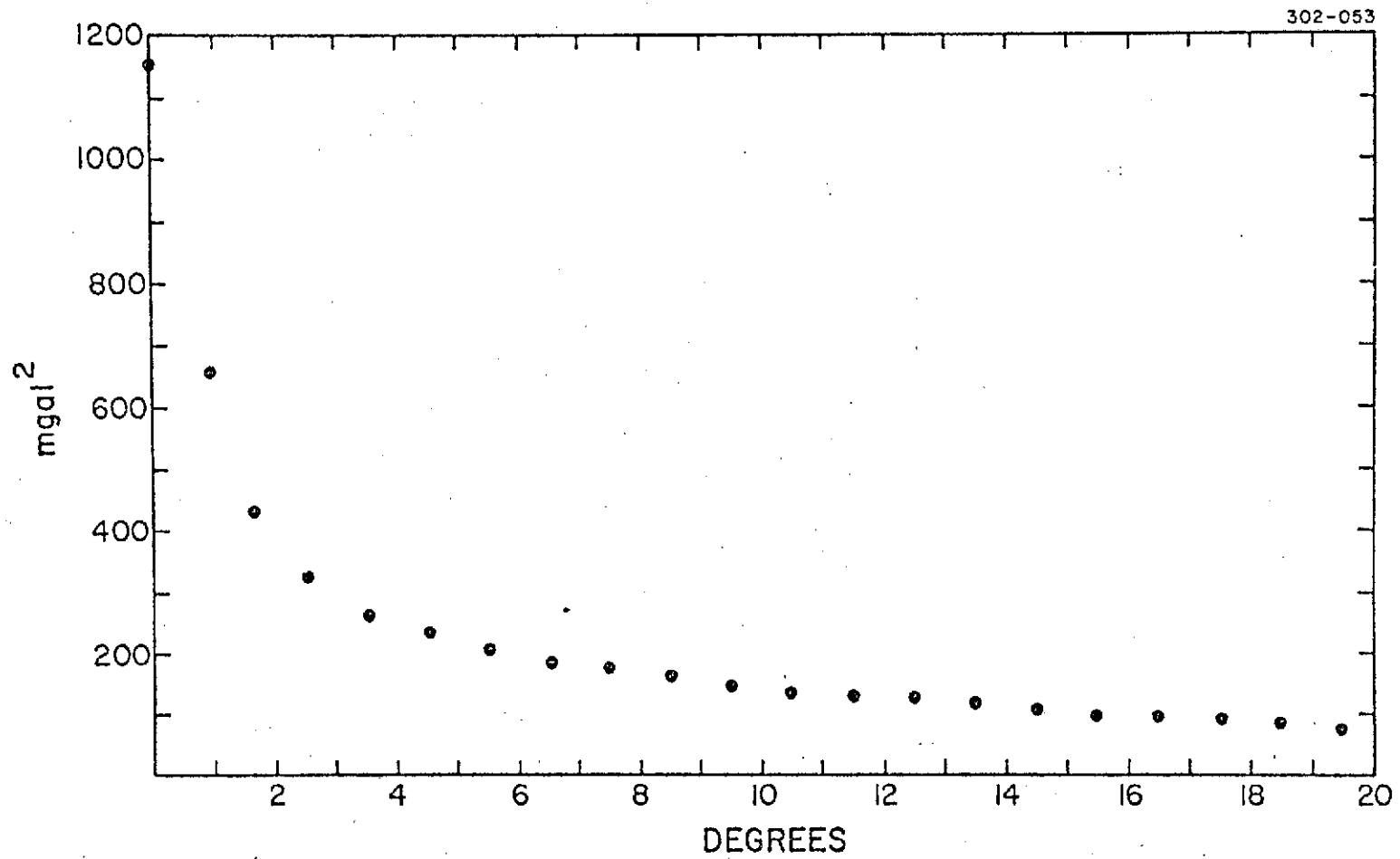
Fig. 4. The covariance function of 19,328 1° × 1° mean gravity anomalies.
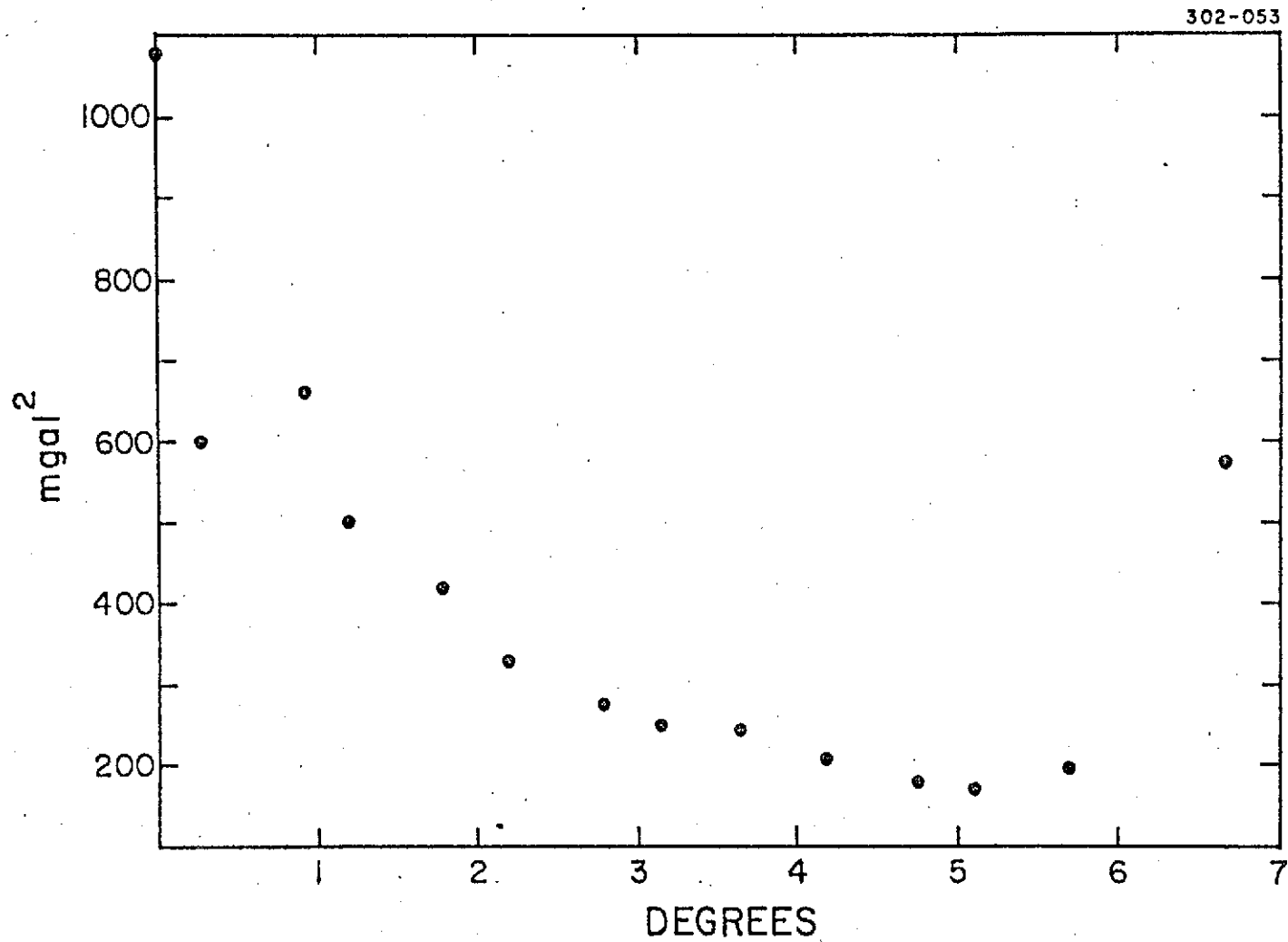
Fig. 5. The block covariance function of unit gravity anomalies.
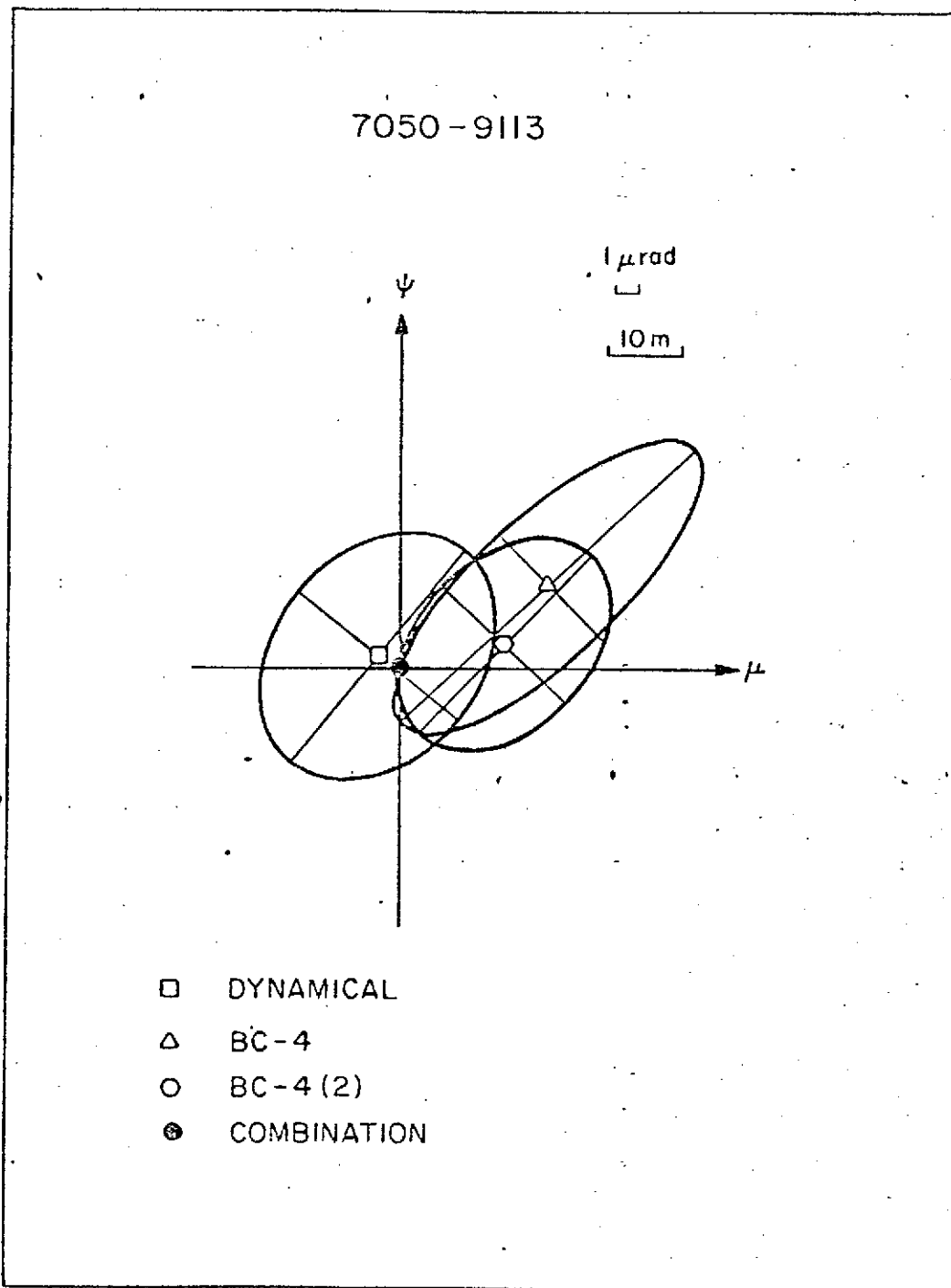
Fig. 6. Comparisons of interstation directions from the combination, dynamical, and geometrical solutions. Each of the two geometrical solutions yields two directions. BC-4 (2) and geometrical (2) are the directions obtained from the network adjustment. ψ is in the direction of increasing declination, and μ is in the direction of increasing right ascension.
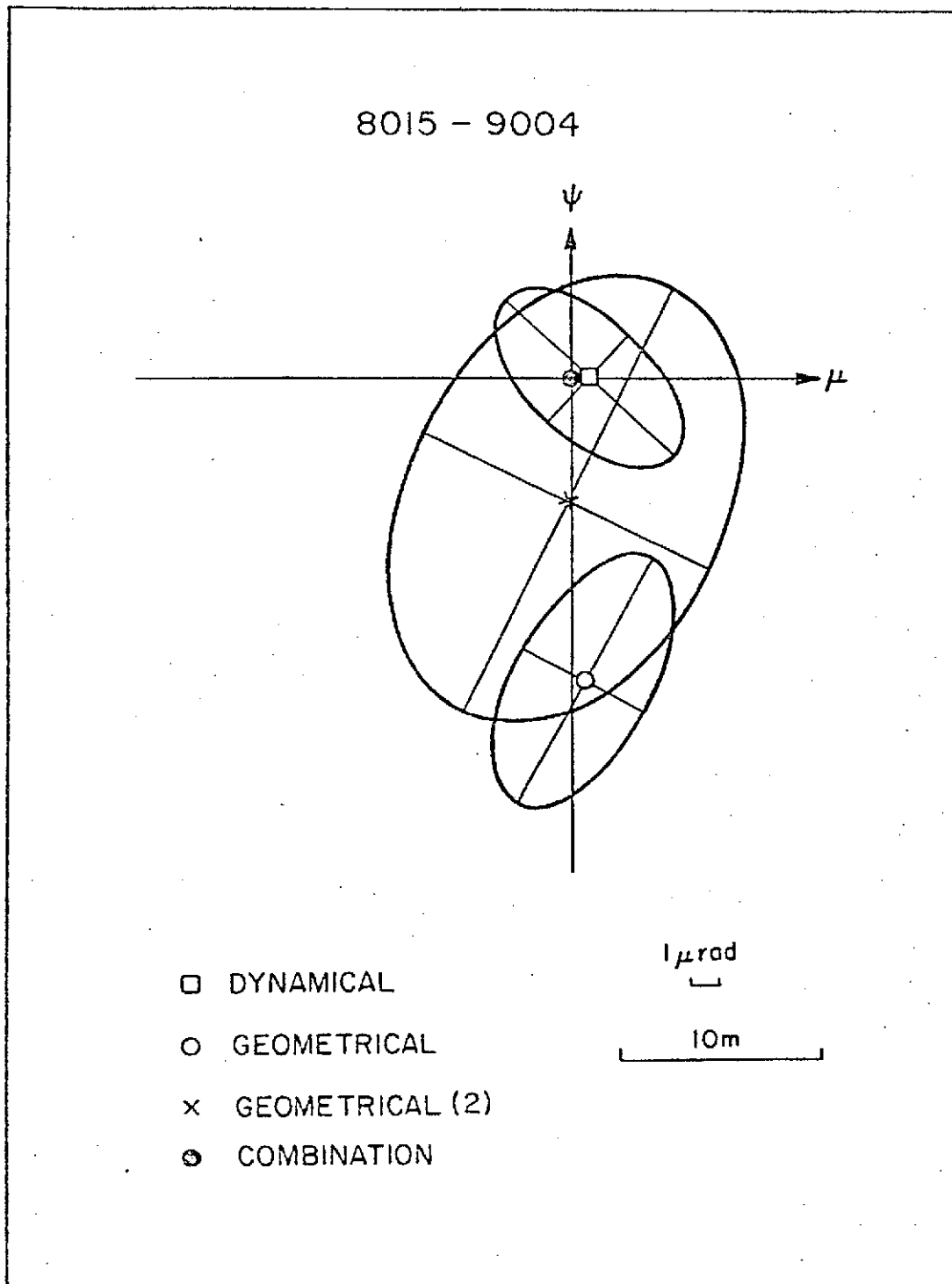
Fig. 6. (Cont.)

9001 – 9010
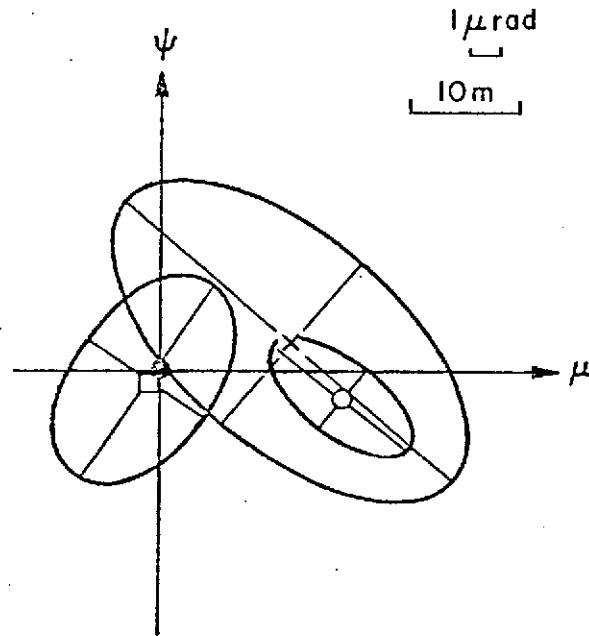
□ DYNAMICAL

○ GEOMETRICAL

× GEOMETRICAL (2)

⊕ COMBINATION

Fig. 6. (Cont.)
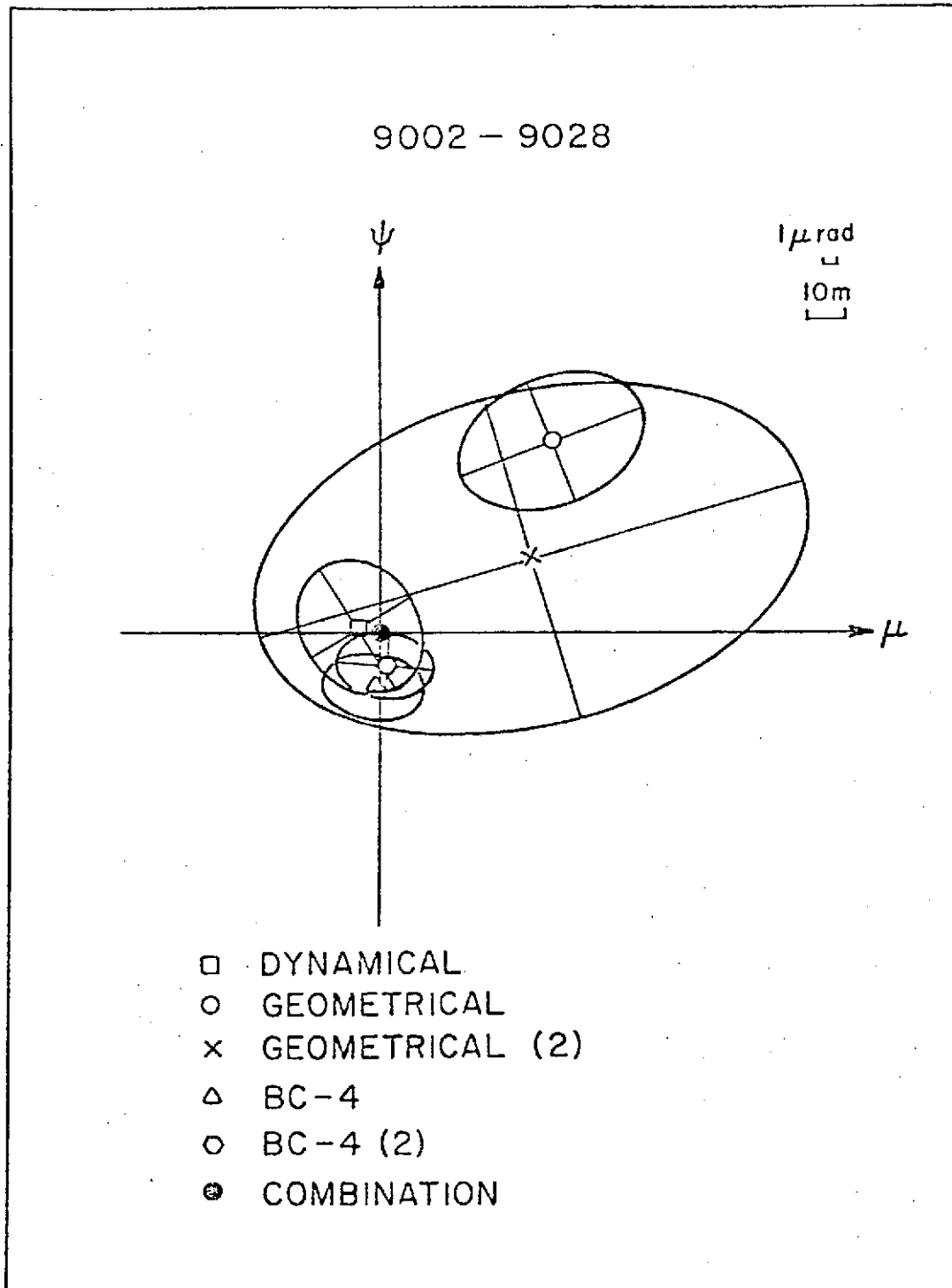
Fig. 6. (Cont.)
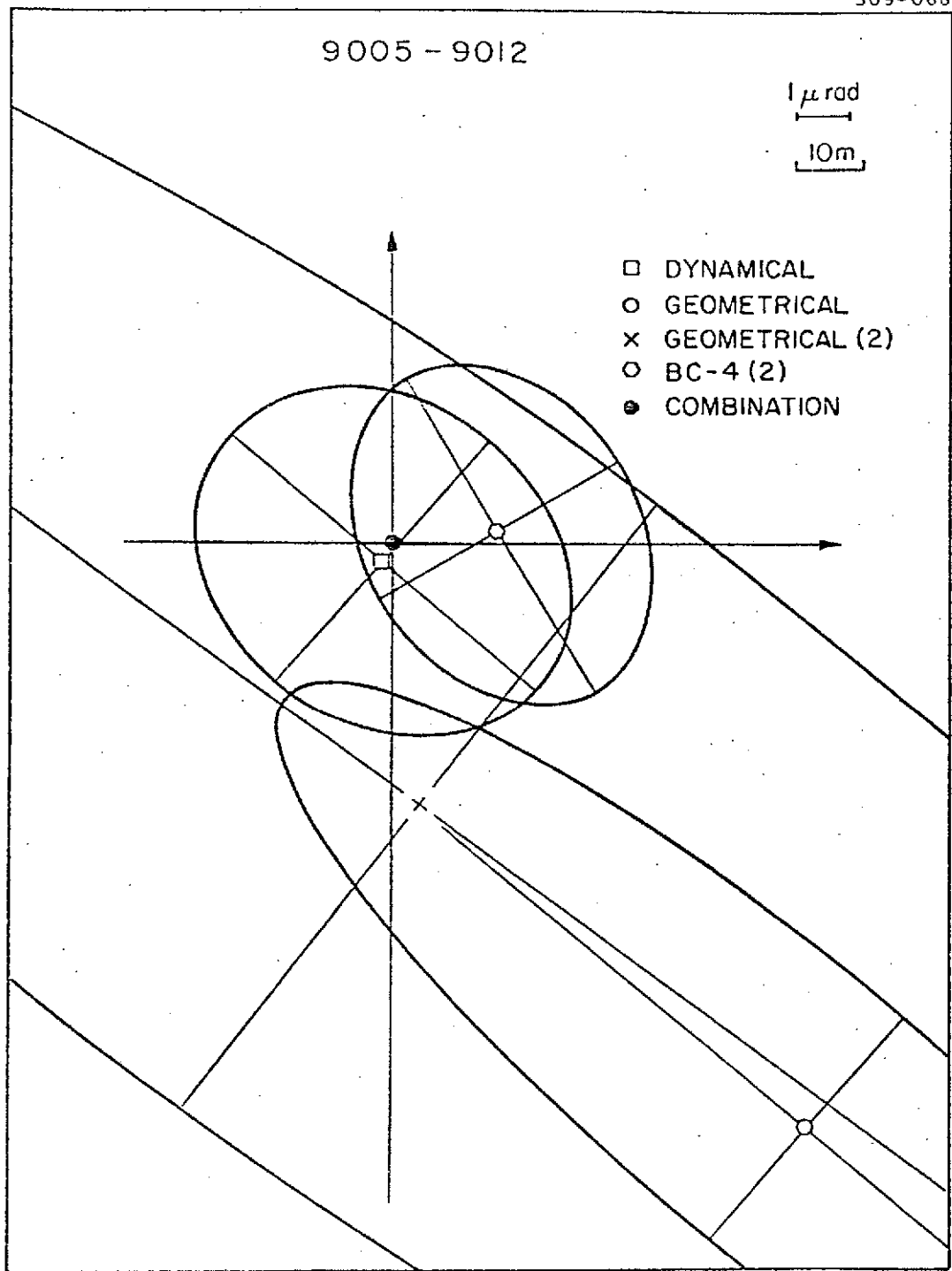
Fig. 6. (Cont.)
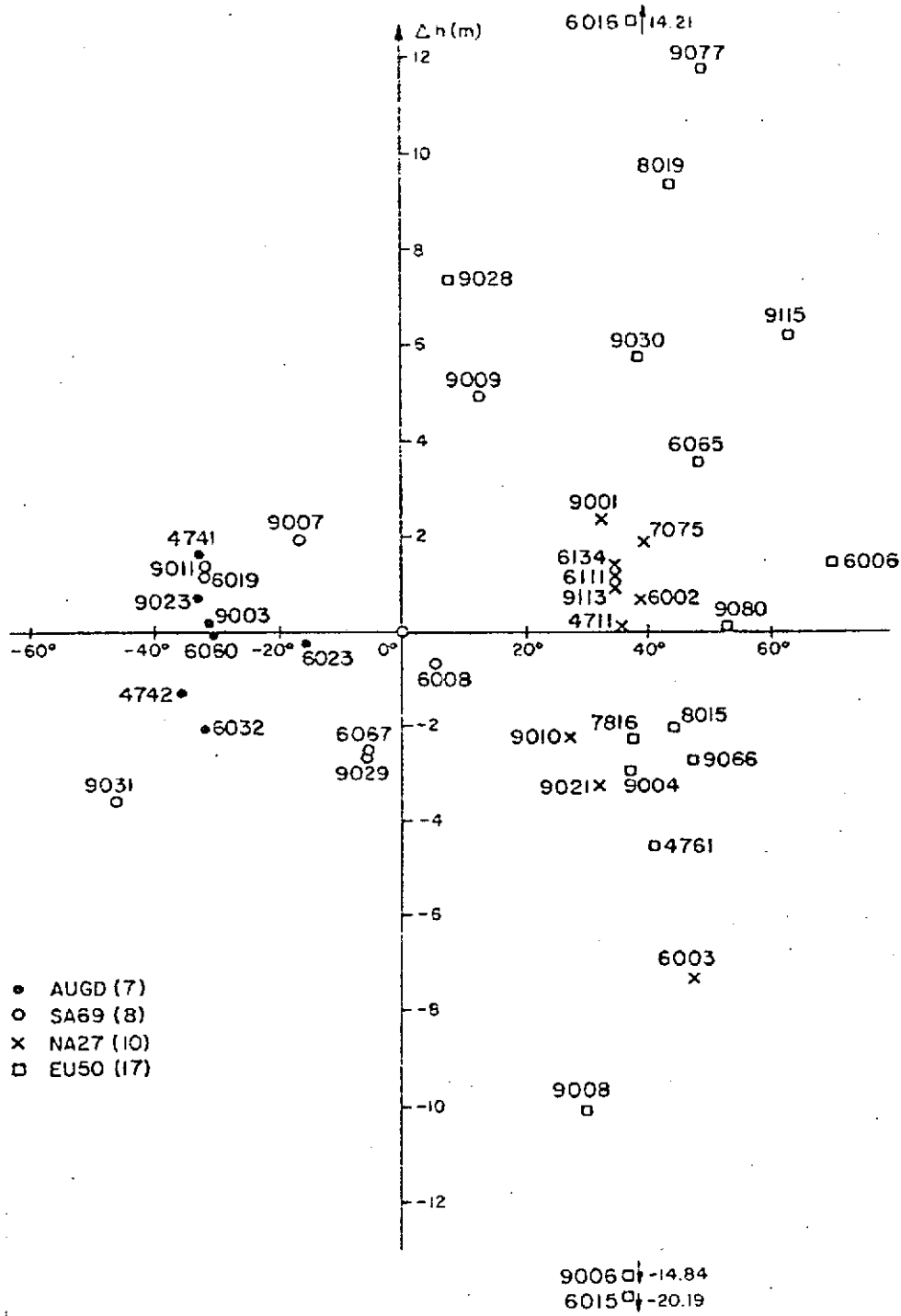
Fig. 7. Geoid-height comparison as a function of latitude $\Delta h = h_{ell} - h_{msl} - N_{datum\ geoid} - \bar{h}_{datum\ mean}$, where h_{ell} is transformed by the appropriate datum-shift parameters. $\sigma_{\Delta h} = 3.98$ m.

88
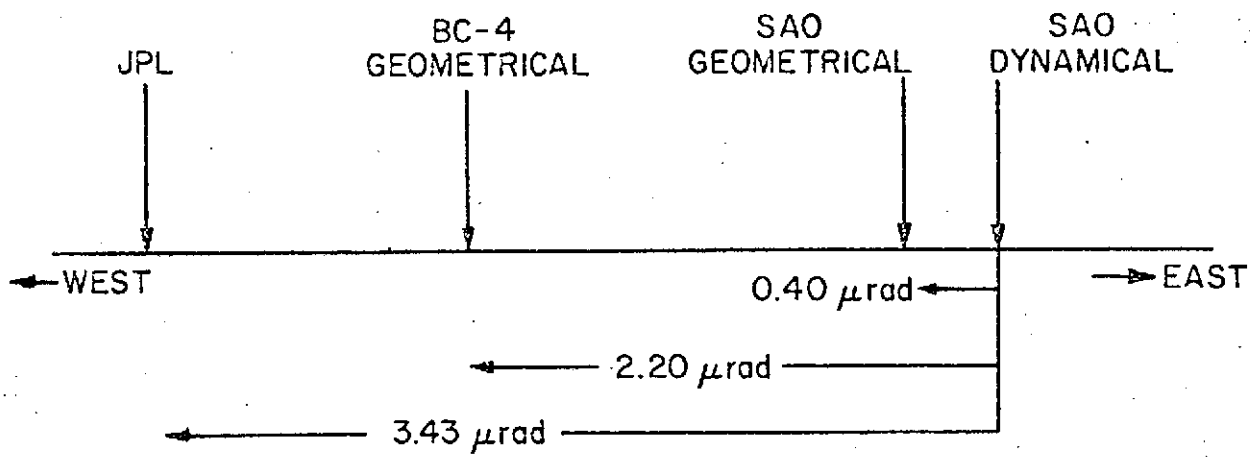
Fig. 8. The relative zero meridians of the different systems.
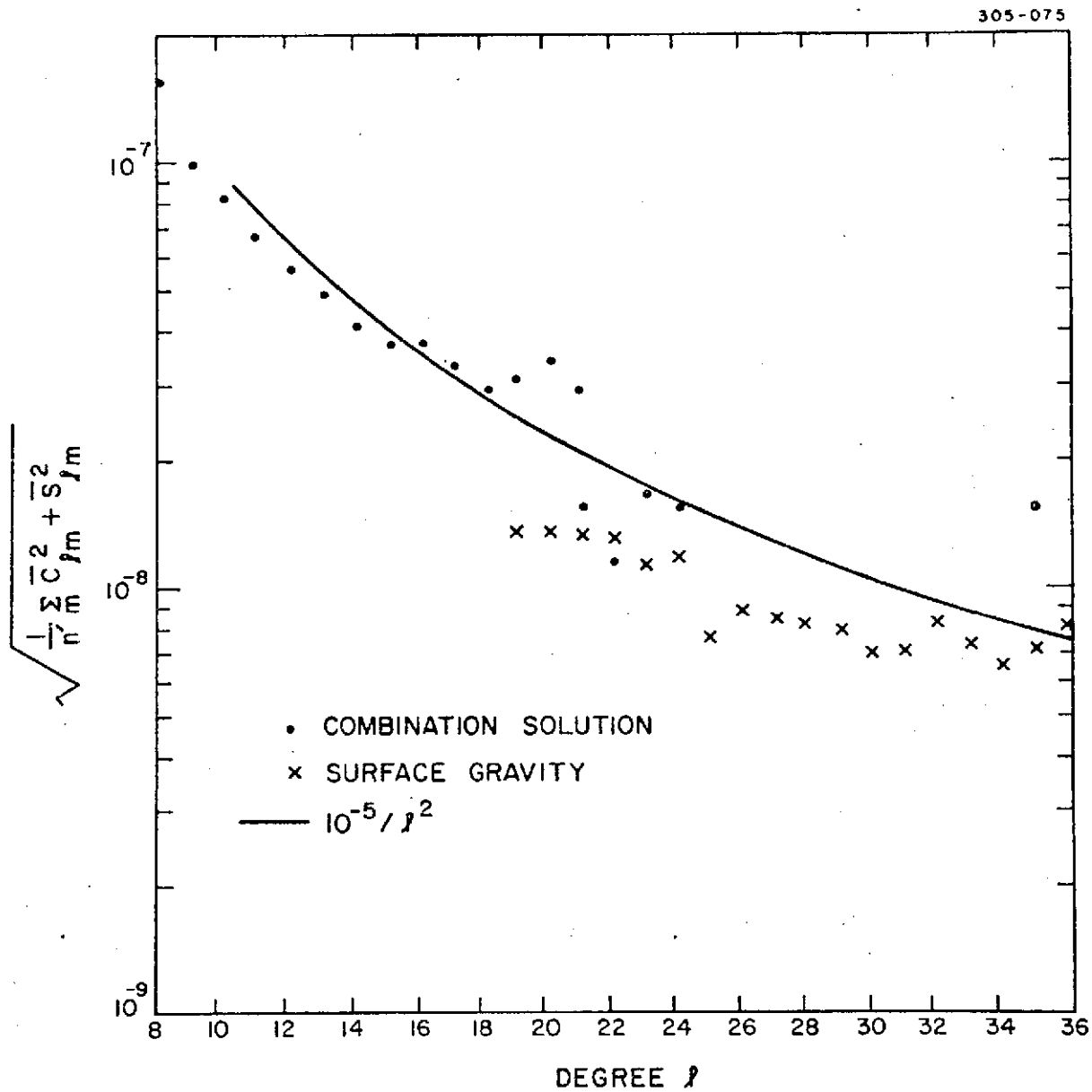
Fig. 9. Mean potential coefficient by degree; n' is the number of coefficients in the sum.
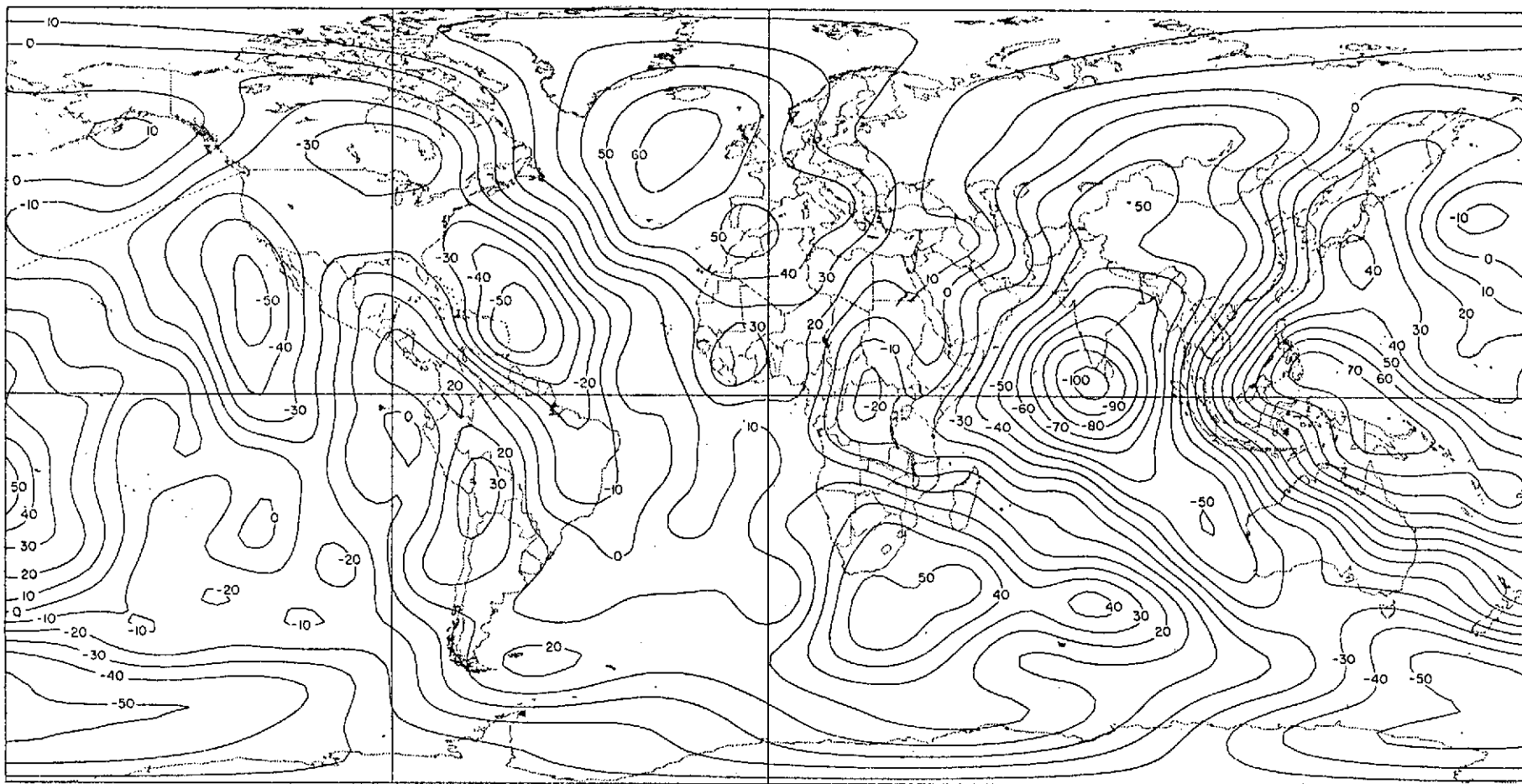
Fig. 10a. SE III geoid height in meters calculated with respect to the best-fitting ellipsoid, f = 1/298.256.
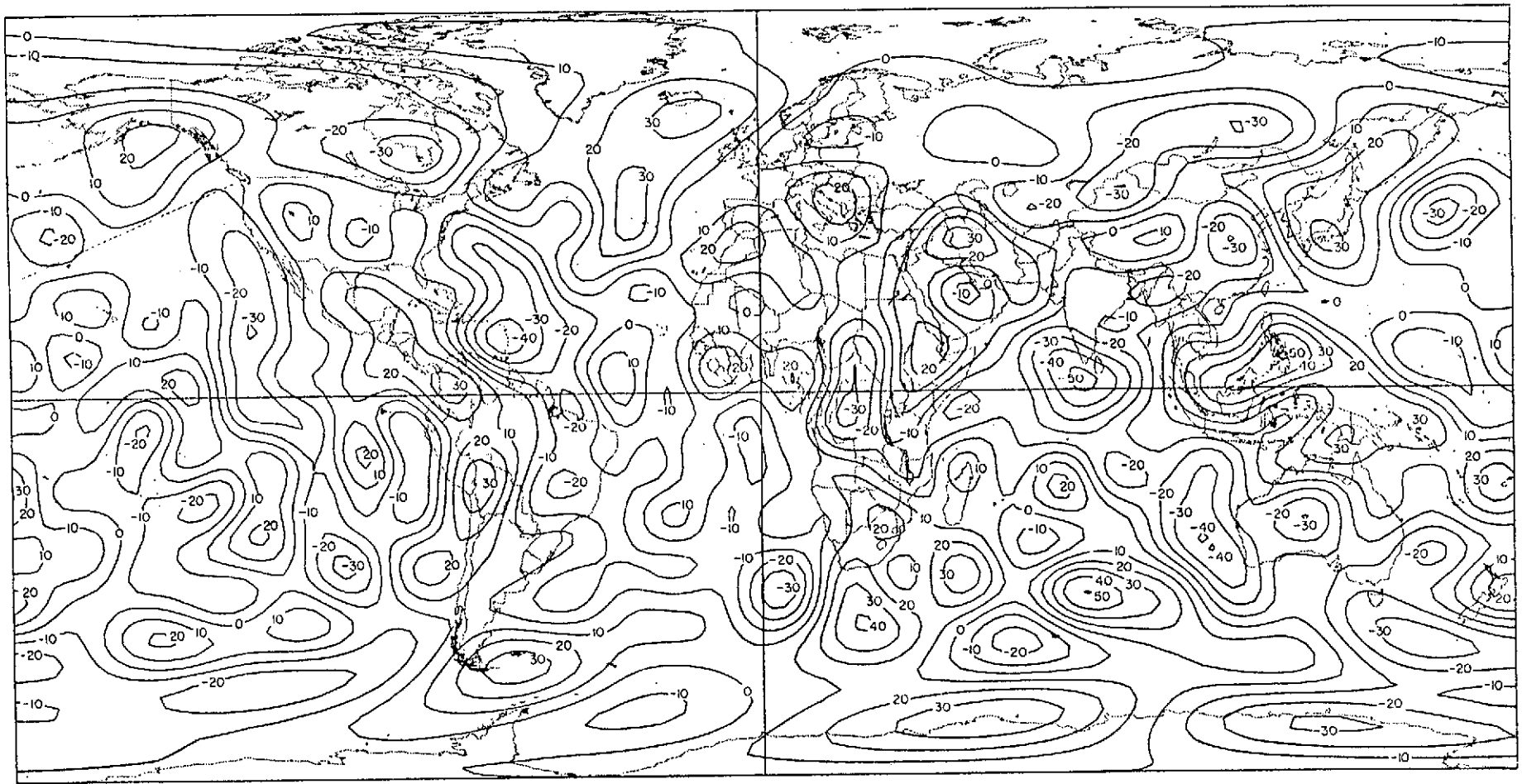
Fig. 10b. SE III gravity anomaly in milligals calculated with respect to the best-fitting ellipsoid, f = 1/298.256.
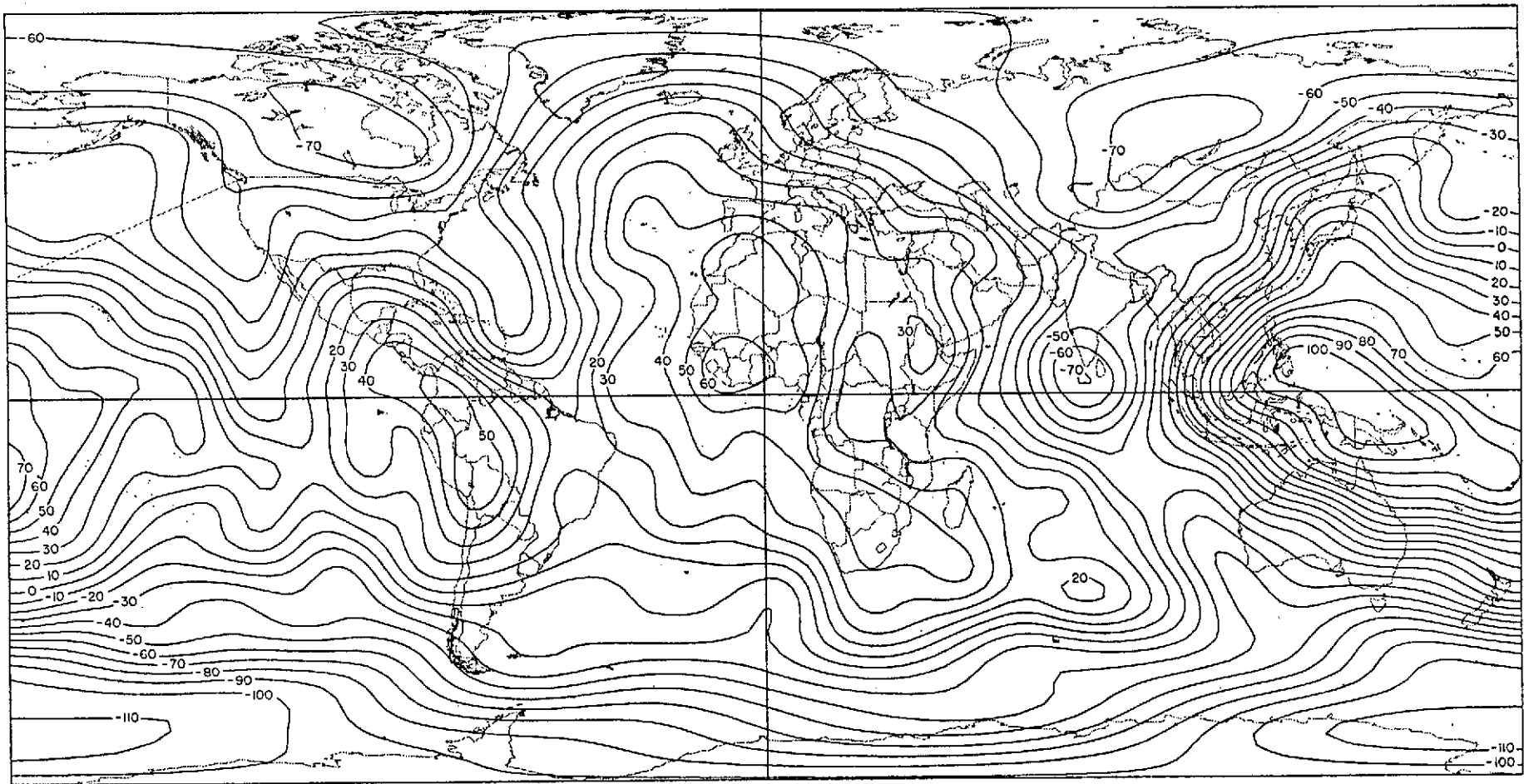
Fig. 10c. SE III geoid height in meters calculated with respect to the hydrostatic ellipsoid, f = 1/299.67.
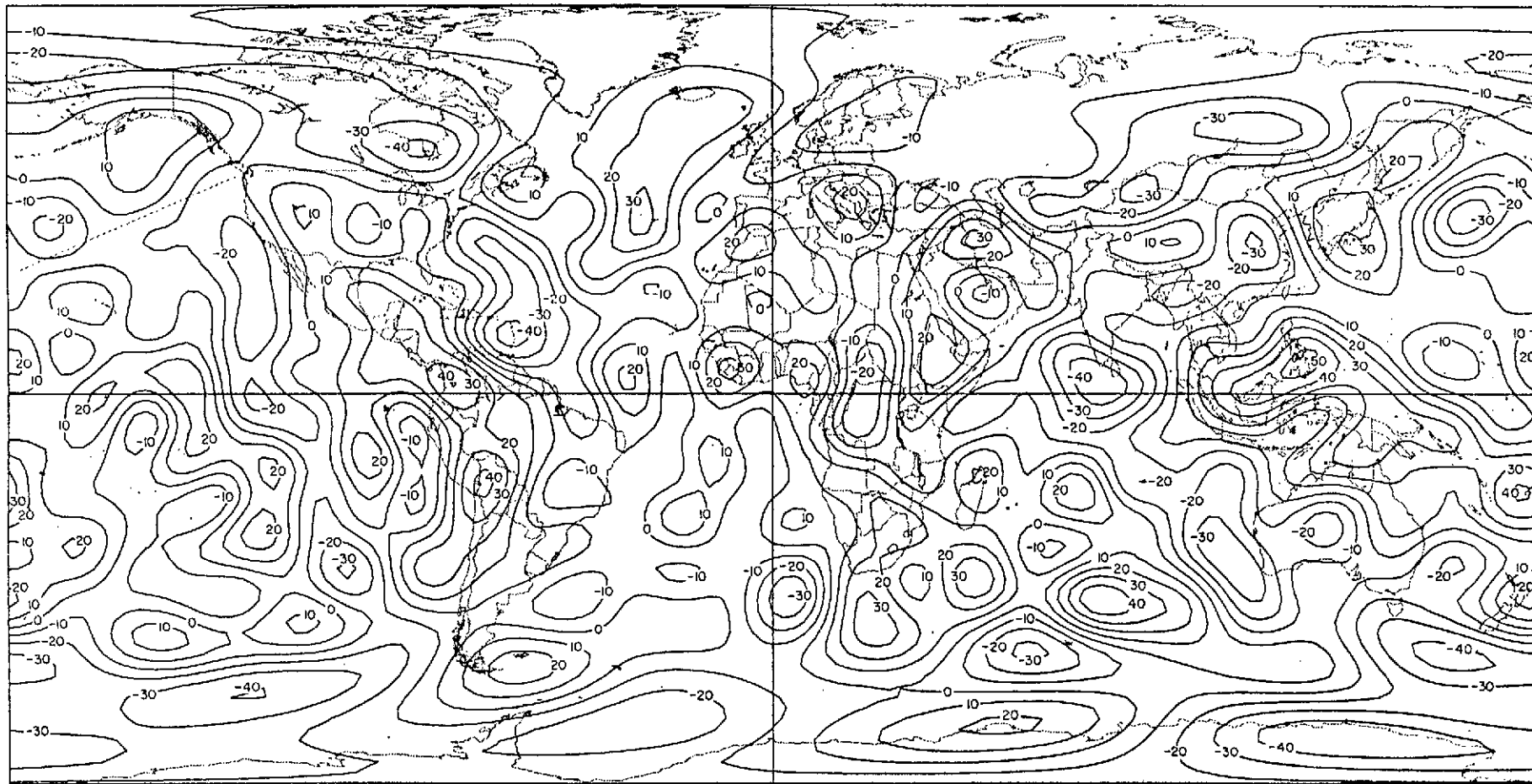
Fig. 10d. SE III gravity anomaly in milligals calculated with respect to the hydrostatic ellipsoid, f = 1/299.67.

Fig. 10e. SE III geoid height in meters calculated with respect to the 5th-degree and order reference surface, $\overline{C}_{\ell m} = \overline{S}_{\ell m} = 0$ if $\ell \leq 5$ and $m \leq 5$.

Fig. 10f. SE III gravity anomaly in milligals calculated with respect to the 5th-degree and order reference surface, $\overline{C}_{\ell m} = \overline{S}_{\ell m} = 0$ if $\ell \leq 5$ and $m \leq 5$.

Fig. 11. Free-air gravity anomalies for North America at latitude 37°5.

Fig. 12.   Free-air gravity anomalies for North America at longitude −82.°5.

...

305-075

Fig. 13. Free-air gravity anomalies for the Indian Ocean at latitude -2°.5.

Fig. 14. Free-air gravity anomalies for the Indian Ocean at longitude 64°5.

305-075

Fig. 15. Free-air gravity anomalies; profile at $\phi = 2°5$.

LIST OF ILLUSTRATIONS

Fig. 10e. SE III geoid height in meters calculated with respect to the 5th-degree and order reference surface, $\overline{C}_{\ell m} = \overline{S}_{\ell m} = 0$ if $\ell \leq 5$ and $m \leq 5$.
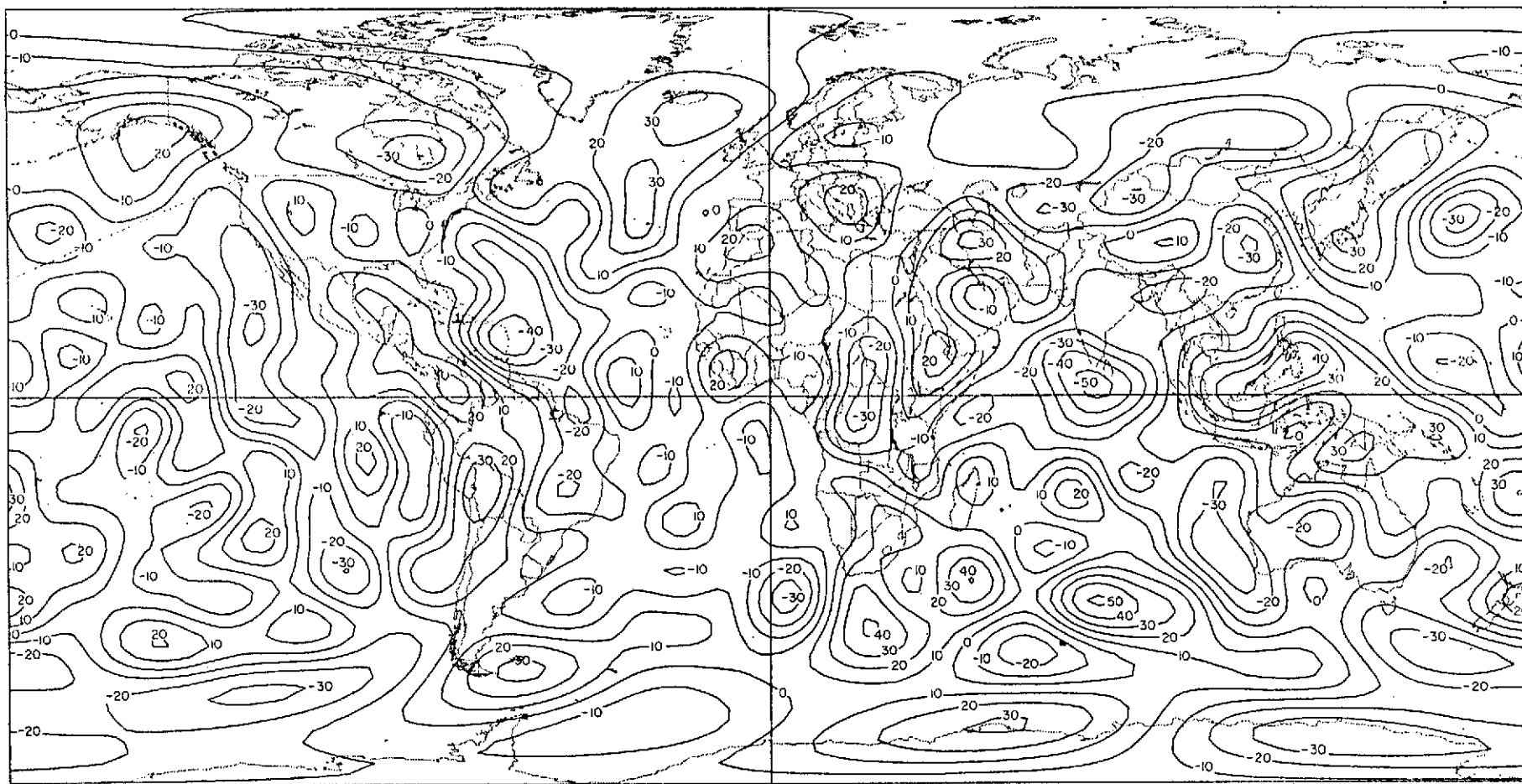
Fig. 10f. SE III gravity anomaly in milligals calculated with respect to the 5th-degree and order reference surface, $\overline{C}_{\ell m} = \overline{S}_{\ell m} = 0$ if $\ell \leq 5$ and $m \leq 5$.

Fig. 11. Free-air gravity anomalies for North America at latitude 37°5.

Fig. 12. Free-air gravity anomalies for North America at longitude -82°5.

Fig. 13. Free-air gravity anomalies for the Indian Ocean at latitude -2°5.

Fig. 14. Free-air gravity anomalies for the Indian Ocean at longitude 64°5.

Fig. 15. Free-air gravity anomalies; profile at $\phi = 2°5$.